A Comprehensive Overview on Biochar-Based Materials for Catalytic Applications

catalysts

MDPI

Review

A Comprehensive Overview on Biochar-Based Materials for Catalytic Applications

Mattia Bartoli [1,2], Mauro Giorcelli [2,3] and Alberto Tagliaferro [2,3,4,*]

[1] Center for Sustainable Future, Italian Institute of Technology, Via Livorno 60, 10144 Turin, Italy; mattia.bartoli@iit.it
[2] Consorzio Interuniversitario Nazionale per la Scienza e Tecnologia dei Materiali (INSTM), Via G. Giusti 9, 50121 Florence, Italy; mauro.giorcelli@polito.it
[3] Department of Applied Science and Technology, Politecnico di Torino, C. so Duca degli Abruzzi 24, 10129 Turin, Italy
[4] Faculty of Science, OntarioTech University, Simcoe Street North, Oshawa, ON L1G 0C5, Canada
* Correspondence: alberto.tagliaferro@polito.it; Tel.: +39-011-0907347

Abstract: The development of heterogeneous catalysts is one of the pillars of modern material science. Among all supports, carbonaceous ones are the most popular due to their high surface area, limited cost, and tunable properties. Nevertheless, materials such as carbon black are produced from oil-derived sources lacking in sustainability. Pyrolytic carbon produced from biomass, known as biochar, could represent a valid solution to combine the sustainability and performance of supported catalysts. In this review, we report a comprehensive overview of the most cutting-edge applications of biochar-based catalysts, providing a reference point for both experts and newcomers. This review will provide a description of all possible applications of biochar-based catalysts, proving their sustainability for the widest range of processes.

Keywords: biochar; thermal catalysis; electrochemical catalysis; heterogeneous catalysis

Citation: Bartoli, M.; Giorcelli, M.; Tagliaferro, A. A Comprehensive Overview on Biochar-Based Materials for Catalytic Applications. *Catalysts* **2023**, *13*, 1336. https://doi.org/10.3390/catal13101336

Academic Editor: Vladimir Mordkovich

Received: 31 August 2023
Revised: 28 September 2023
Accepted: 29 September 2023
Published: 30 September 2023

1. Introduction

Since the early days of chemical industrial production, large-scale production has relied on the use of catalysts to facilitate and optimize most chemical conversions [1]. As proved by empirical results, heterogeneous catalytic systems show a combination of properties that perfectly match the industrial requirements (i.e., recyclability, activity, and recoverability) [2]. Across the history of industrial catalysis, carbon-supported catalysts (CSCs) have played a major role since the development of the Lindlar catalyst [3], which marked the history of industrial processes. Since the first steps, CSCs have spread out in several industrial applications due to their possible combination with several single or multiple metal centers that are able to exploit the catalytic effect (i.e., palladium [4], platinum [5], rhodium [6], and ruthenium [7]) and the high surface area and physical and chemical stability of the support [8]. The possibility of producing multi-site materials allowed the creation of real conversion platforms able to exploit complex chemical pathways. The clearest example is represented by the electrocatalytic applications in which CSCs with multiple active sites allowed the conversion of carbon dioxide to alcohols through intermediates such as formic acid without requiring multiple-stage reactors [9] or reducing the loading of costly species by using cheap metals such as iron [10]. After the selection of CSCs, the morphological, physical, and chemical properties of the carbon support are key features for the production of carbon-supported catalysts [11,12]. The surface properties of CSCs are a matter of great relevance, affecting both active site distribution and catalyst–reagent interactions [12].

The use of pristine nanosized carbon-based species represented a key advancement for CSC [13], enlarging the carbon black-supported species and introducing the use of

graphene derivatives or carbon nanotubes [14], reaching fields such as biomedicine in which high-tech materials represent critical and mandatory innovations [15–17]. Nevertheless, these materials are still far from reaching large-scale applications due to handability, cost, and productive limitations [18]. During the last decades, the rise of social concerns for environmental preservation has also driven the development of greener solutions for the production of CSCs based on engineered waste or biomass-derived materials [19]. This field is quite promising, but a fully engineered waste or biomass-derived catalytic support is still far from being able to match all the properties of a traditional CSC considering stability and utilization range [20]. Interestingly, carbon produced from the thermal degradation of biomass, known as biochar (BC), has attracted great interest as a replacement for carbon black for plenty of applications, such as composites production [21–27]. The BC properties can be easily tailored by simply tuning the production conditions, increasing its electrical [28–32] or thermal [33–35] conductivity, and modifying its morphology [36,37]. The great tunability [38], low cost [39], and environmental impact [40] have promoted the use of BC in the realm of CSCs far beyond the more cutting-edge and high engineering materials, reaching remarkable achievements [41–43]. An additional feature of BC is its easy dispersibility in polymeric matrix together, the "shuttle" effect for nanofillers such as carbon nanotubes [44]. Nevertheless, BC production is struggling to reach full maturity due to geographical constraints and the strong dependency of the economy on its final application [45]. BC-supported catalysts (BCSCs) can be a solid solution to reach the breakthrough that will allow the consolidation and spread of BC-based platforms due to the high cost of the CSCs, mitigating their environmental impact. Actually, BCSCs have found an active role in the mitigation of environmental pollution, both in adsorption [46] and in degradative processes [47–49]. Nevertheless, the BCSCs cannot be limited to the environmental field in order to promote the development of a large, resilient, and productive network. A great deal of work has already been carried out on BCSCs, and a reference point is needed to establish critical discussions on which is the most promising catalytic field for the use of BCSCs.

In this review, we provide a clear and complete picture of all possible uses of BCSCs, focusing on the strong and weak points for each catalytic route discussed and clearing up the possibility of the utilization of BCSCs in several catalytic applications as a solid replacement for traditional CSCs.

2. Engineering the BC for Catalysts Production

BC is derived from biomass through thermochemical cracking using different methods such as torrefaction, pyrolysis, and gasification. The primary difference between them lies in the temperatures reached during the process. The temperature achieved during torrefaction ranges between 200 and 350 °C. Torrefaction conversion technology avoids proper carbonization of the material, reaching only a low degree of biomass degradation [50]. BC produced at such low temperatures contains up to 50 wt.% of carbon, with remarkable yields of up to 70% [51]. Nevertheless, the limited processing temperature avoids full carbonization, promoting only a limited condensation process with breakage of lignocellulosic components.

Proper carbonization occurs at temperatures higher than 400 °C under the so-called pyrolytic condition in an oxygen-poor atmosphere [52] using several kinds of heating technologies [53–55] and reactors [56]. Alternatively, techniques based on the use of liquid [57] or oxidant [58] environments can be used, but they generally have been employed for liquid or gas fuel applications.

The formation of BC takes place through several steps during the carbonization of biomass. At first, the biomass feedstock lost adsorbed water in a temperature range of 100–1130 °C, while the proper breaking process of major components starts at 400 °C and becomes complete at around 550–600 °C [52]. Nevertheless, this temperature range is far from the one required for graphitization, and BC produced using pyrolytic temperatures up to 600 °C is still rich in functional groups but displays a poor degree of graphitization [59].

The advanced graphitization of BC takes place at temperatures higher than 800 °C [60] and never reaches pure graphitic status as it is classified as non-graphitizable carbon according to the Franklin definition [61].

The balance between graphitization and residual groups is a matter of complexity, and it is related to the selection of BC productive conditions. These are strictly connected to the BC final use, and their choice is used to tailor key parameters ranging from grindability to physicochemical properties (i.e., residual functional groups, conductivity, and degree of carbonization) [62]. Among all parameters, the processing temperature plays a major role, and its effect can be monitored through the Van Krevelen graph (see Figure 1) plotting the molar ratios H/C versus O/C.

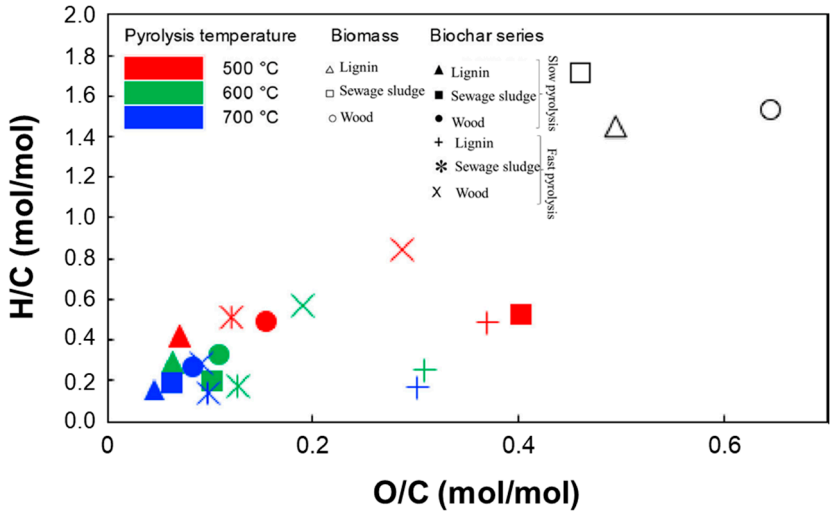

Figure 1. Van Krevelen graph showing relevance of processing temperature. Figure is adapted and reprinted with all permission (CC BY-NC-ND 4.0) from Bartoli et al. [63].

The Van Krevelen plot is very useful for correlating the heteroatom residues on BC with the process temperature and to deduce this parameter through a simple elemental analysis. Nevertheless, a more detailed evaluation of fine parameters such as the carbon defectiveness and the species exposed on the surface is required for BCSCs. These analyses are generally carried out using advanced techniques such as Raman and infrared spectroscopies [60], electron microscopy [64], and X-ray investigation techniques [30,65].

The production of BCSCs is a matter of great complexity, and the use of pristine BC is not an elective choice due to the intrinsic lack of BC catalytic activity [66,67]. The engineering processes of BC are numerous and comprise two approaches, one based on the insertion of functionalities on the BC surface and the other based on BC tailoring with active micro- and nanostructures.

The well-established functionalization of BC has found its foundations in the procedures developed for tailoring carbonaceous structures for the production of catalysts [68] and absorbers [69].

The first relevant tailoring route is based on the insertion of heteroatoms (i.e., sulphur and nitrogen) in the BC matrix to modify the electronic properties and the reactivity of the vacancies produced in the carbon skeleton [70–72]. A simple route to enforce this approach is based on the production of BC through direct pyrolytic conversion of heteroatom-rich materials such as chitin [73]. Alternatively, more complex procedures can be used, ranging from mechanochemistry-based [74] to impregnation [75] and washing with several organic and inorganic solutions [76–80]. The covalent conjugation with metal–organic frameworks or with polymeric chains is also used to modulate the interfacial properties of BC [81,82]. An interesting tailoring process is represented by BC activation. BC activation induces a great increment in the specific surface area up to several hundreds of m^2/g [83], removing the trace of unreacted volatile organic matter and tar from BC particles [84]. The

activation process can be either physical or chemical, depending on the activation agents used. Physical activation is performed by using a process temperature higher than 800 °C in the presence of oxidant gases such as steam, CO_2, H_2O, or NH_3 [85]. While physical activations are relatively clean approaches, they require long process times and elevate energy consumption [86]. Chemical activations are considerably faster, but they require the use of large amounts of harmful agents such as oxidant acids [87,88], alkali [89,90], carbonates [91,92], or peroxides [93–95].

BCSCs can also be produced by using engineered BC obtained by the growth of deposited structures on their surfaces. Carbon tailoring represents an interesting route to modulate the BCSC activity for all the electrochemical processes by inserting carbon nanostructures, as reported by Zhang et al. [96]. The authors used chemical vapor deposition (CVD) to grow carbon nanotubes on BC produced from nuts, while other authors introduced micrometric needles or semi-spheres on cellulose-derived BC [97].

CVD was used for the deposition of several metal structures onto polymers [98] or carbon matrix [99,100], but it is not the most used technique for metal tailoring in BC. BC is mainly tailored through solvothermal routes, calcination, and carbothermal reduction. Solvothermal routes are useful, but they lack deposition uniformity and require a calcination step to fix the inorganic species onto BC, as described by Zeng et al. [101]. On the contrary, carbothermal approaches directly anchor the inorganic structures on the BC through the partial reduction of inorganic precursors using BC itself as a reducing agent [102], resulting in a massive alteration of the BC morphology, as mentioned in several papers [103,104].

As summarized in Table 1, the choice of BC engineering technique should be carried out by balancing the application of BCSCs with the cost-effectiveness of the route selected.

Table 1. Advance and disadvantages of engineering BC techniques.

Technique	Modification	Advantages	Disadvantages
Tune the pyrolysis parameters [105,106]	▪ Adjustments of residual functionality ▪ Increase in BC conductivity	▪ Simple approach ▪ It can be used with all the feedstock	▪ Unable to insert any new functionality
Pyrolysis of heteroatom-rich feedstock [107]	▪ Heteroatom insertion	▪ Simple approach	▪ Limited to specific feedstock
Activation [108]	▪ Increase in specific surface area ▪ Remove of tar ▪ Insertion of oxygen and nitrogen-based heteroatoms	▪ It can be use with all BC. ▪ Physical activation does not require any specific reagent other than activation gas. ▪ Chemical activation can improve the specific surface area up to 1 order of magnitude and simultaneously passivate the BC surface.	▪ Requires a post treatment step ▪ Physical activation is an energy consumption route and require long process time. ▪ Chemical activation requires the use of great amounts of unfriendly reagents
Organic Tailoring [109]	▪ Insertion of residues, carbon structure or polymeric chains on BC surface	▪ Great control ▪ Highly tunable	▪ Require a post-treatment step ▪ Expensive ▪ Not useful to exploit BC as cheap material

Table 1. *Cont.*

Technique	Modification	Advantages	Disadvantages
Inorganic Tailoring [110]	▪ Insertion of inorganic micro- and nanostructure on BC	▪ Great control ▪ Highly tunable ▪ Great catalytic activity promoted by inorganic species	▪ Require a post-treatment step ▪ Expensive ▪ Necessary for the great part of BCSC production ▪ Possible inorganic leaching

3. Nanostructured and Nanosized Carbon Materials: Catalytic Applications

3.1. Thermochemical Based BC Catalytic Systems

3.1.1. Hydrogenation of Organic Compounds

The oldest field of application for supported catalysts is the hydrogenation of organic compounds since the development of Lindlar catalysts [3]. The quest for highly active green catalysts has been a vital research field, and BCSCs can play an interesting role in the fulfillment of these aims by providing a combination of tuneability and toughness. Furthermore, BCSCs show better recoverability compared to traditional catalysts supported on fine activated carbon that are hard to filter away, while micrometric BCSCs are considerably easier to recover.

Santos et al. [111] tested the relationship between the textural properties of BCSCs containing ruthenium and their activity in the reduction of monomeric sugars. The authors clearly report a direct relationship between the number of residual groups and the BCSC activity in the production of hexitols, which reached up to 95%. They suggested that this behavior was due to the role of each residual group as a possible active center, reporting also the crucial effect of metal sites' homogenous dispersion, as also reported for other BCSCs [112,113]. The relevance of BC surface modification was enlightened by Wang et al. [114] in the hydrogenation of 1-chloro-2-nitrobenzene using nickel-supported catalysts. The authors simultaneously introduced both hydrophilic and hydrophobic sites through a combination of chemical activation and thermal annealing, boosting the unsaturated bond reduction activity.

Similarly, Dou and co-workers [115] evaluated the effect of BC porosity by depositing palladium nanoparticles onto chemically activated cellulose-derived BC. The results showed that activated BC overwhelmed the activity and recyclability of untreated BCSCs working even at lower temperatures. Similar correlations were reported for the reduction of phenols using potassium hydroxide-activated BC and nickel/cobalt-active species [116].

The insertion of specific heteroatoms was reported by Marques et al. [117] using copper supported onto vineyard pruning waste derived from BC doped with nitrogen. The authors proved the beneficial effect of nitrogen sites in the reduction of furfural to furfuryl alcohol, reaching a conversion of up to 80% at 160 °C. As mentioned above, the insertion of heteroatoms can be performed by processing specific materials such as sewage sludge [118] or even by adsorbing metal ions from contaminated water and using the resulting BC as BCSCs [119].

BCSCs can also be used for the hydrogenation of biomass [120], biomass-derived fuels [121], and chemicals [122] for the creation of fully biomass-based sustainable platforms. This is one of the most interesting possibilities related to BCSCs due to their inclusion in fully biomass-based value chains. Van den Bosch et al. [123] reported the hydrotreatment of birchwood lignin by using BCSCs containing both ruthenium and palladium, showing the ability of the material to demethoxylate the guaiacol moieties at 240 °C while activated carbon-supported catalysts required over 300 °C. Noble metals can be replaced by non-noble species such as nickel, obtaining comparable deoxygenative performance with only a small decrease in activity [124–126]. BCSCs have also found applications in the upgrading of bio-oils, the liquid fractions produced from the pyrolysis of biomass [127,128]. These species

are very complex in composition, containing up to hundreds of compounds, a high amount of oxygen, and acidic molecules. BCSCs have been used for the hydrodeoxygenation of bio-oils by directly mixing them with the pyrolytic feedstocks or in post-pyrolysis experiments. The co-pyrolytic approach is particularly interesting for the simple realization but involves a very complex reaction pathway including cracking, rearrangements, and hydrogen transfers [129,130], while the post-treatment deals with a simple reactivity but several deactivation issues to the composition of native bio-oils [121].

3.1.2. Oxidation of Organic Compounds

Among the thermal catalytic processes, the use of BCSCs for the oxidation process is the most widely investigated due to their widespread application in water treatment for pollution removal [131] and advanced desulphurization [132]. The oxidative process of organic compounds mediated by BCSCs is not carried out using air or oxygen due to the possible advanced oxidation of the BC matrix, but it is generally performed using Fenton and Fenton-like reactions. Traditionally, a Fenton reaction involves the production of reactive oxygen species through the decomposition of oxygenated water in the presence of Fe(II) salts [133], with a well-known mechanism based on the equilibrium between Fe(II)/Fe(III) species [134] and similar routes for Fenton-like reactions based on the use of Fe(III) catalysts [135,136]. These reactions were originally developed as homogenous catalytic reactions [137], but the production of heterogeneous catalysts has rapidly gained relevance [138]. Manjuri Bhuyan et al. [139] developed BCSCs based on Fe_3S_4 that were able to promote the rapid conversion of Fe(III) to Fe(II), combining the advantageous handability of Fenton-like catalysts with the high reactivity of Fenton ones. This was due to the in situ formation of sulphonyl radicals that allowed a rapid radical transfer to carbon support, regenerating the Fe(II) sites.

As reported by Devi et al. [140], BC has shown remarkable stability under Fenton model conditions for the degradation of naphthenic acids. The authors reported a higher oxygenated water decomposition rate compared with activated carbon with a maximum radical concentration of up to 182 mg/L that allowed these systems to operate under real-world operating conditions. Mixed results were obtained by comparing the oxidation of tetracycline using chemically activated BC produced by potassium permanganate, potassium hydroxide, or phosphoric acid and different feedstocks [141]. The authors showed that the feedstock plays a minor role while the activation process could enhance the reagent adsorption, as in the case of permanganate treatment, and the catalytic activity, as in the case of potassium hydroxide, depending on the functionalities introduced, as also reported for BCSCs used for ozonation of wastewaters [142]. Additionally, the well-known catalytic effect of aluminum doping can be exploited by producing BCSCs using aluminum-rich feedstock and water sludge [143,144] or red mud [145]. Alternatively, the urea-oxygenated water route can be followed with remarkable results using simple Fenton-like BCSCs [146]. The approach allowed the formation of a wide range of reactive oxygen species other than oxygen radicals such as O^{2-} and $^1O_2$, which greatly increased the common Fenton reaction performances [147,148].

The relevance of BCSCs in oxidant catalytic systems has also reached fuel upgrading, in which catalytic oxidative desulphurization has outperformed the traditional desulphurization routes [149].

As reported by Tamborrino et al. [103], iron-loaded coffee-derived BCSCs were synthesized through carbothermal routes and employed to desulphurize a recalcitrant feedstock produced from the pyrolysis of waste tires. The liquid, which contained over 7000 ppm, was treated in mild conditions, reaching a desulphurizaiton of over 60% without any appreciable leaching phenomenon. Similar approaches can be used for the catalytic oxidation of sulphuric acid using BCSCs as a platform for simultaneous adsorption and oxidation processes [150,151] reaching desulphurization over 70% even at room temperature.

Traditional CSCs suffer from great alternation during oxidative catalytic cycles that greatly change their chemical and structural features, avoiding their use as inorganic

support materials. BCSCs can be improved in their activity by the presence of additional oxygen sites, increasing their performances [152,153].

3.1.3. Fischer–Tropsch Process

The Fischer–Tropsch process (FTP) is a well-established chemical route to convert a mixture of carbon monoxide and hydrogen into liquid hydrocarbons, as reported in Figure 2.

$$(1)\ nCO + (2n+1)H_2 \longrightarrow C_nH_{2n+2} + nH_2O$$
$$(2)\ nCO + 2nH_2 \longrightarrow C_nH_{2n} + nH_2O$$

Figure 2. FTP chemical pathway for the formation of (1) saturated and (2) unsaturated hydrocarbon mixtures.

FTP is the most industrially relevant gas-to-liquid fuel technology for the production of an oil derivative analog using reforming gas. Actually, cobalt-containing catalysts represent the state of the art of FTP using an H_2:CO ratio close to 2 [154], but syngas produced from low-quality sources such as biomass can have different compositions [155], requiring the presence of an iron co-catalyst [156]. There are few examples of BCSCs, but the results reported were comparable or better compared to similar catalysts supported on carbon black [157], with the advantage that micrometric BC particles reduce the poisoning of metal centers [158]. Yousefian et al. [159] comprehensively evaluated the relevance of BC feedstock for FTP producing 15 wt.% cobalt supported onto BCSCs using several biomass sources (i.e., rice husk, coconut shell, and algae) using deposition methods. The experiments were run in a fixed-bed reactor at 400 °C with an optimum H_2:CO ratio, comparing the catalytic activity with a common alumina-supported catalyst. The authors reported that the low-ash BC produced from algae displayed better performance, with a conversion of up to 67%. Nevertheless, iron–cobalt BCSCs showed superior performances, as reported by Yan et al. [160]. The authors used a carbothermal reduction approach to form nanosized supported metal catalyst anchoring with a thin layer of iron carbide, reaching conversion up to 95% conversion, a value stable for more than 1500 h of working activity. Alternatively, the modification of BC texture can also improve the output of FTP, particularly after activation [161] or by inserting nitrogen doping. As reported by Bai et al. [162], the presence of pyrrolic functionalities improved the selectivity towards long-chain hydrocarbons due to a better adsorption of CO.

Compared to inorganic-supported catalysts, BCSCs do not suffer from poisoning, and the weak adsorption interaction on their surfaces greatly promotes the efficiency of the hydroformylation process.

3.1.4. Cross Coupling Reactions

The cross-coupling reactions are powerful tools for any synthetic process that requires the formation of new carbon–carbon or carbon–heteroatom bonds [163]. These reactions are possible only in the presence of specific catalytic metal centers [164] that promote mechanisms such as the one schematized in Figure 3.

The catalysts for cross-coupling processes were originally designed as homogenous ones [165], and heterogeneous species are still far less active [166]. Nevertheless, cross-coupling heterogeneous catalysts are still attractive due to their good stability after multiple catalytic cycles. Carbon supports have been proven to be the most promising way to produce them [167]. To the best of our knowledge, only one research study has been reported using BCSCs for performing a cross-coupling reaction. Akay and co-workers [168] performed a solventless Suzuki–Miyaura coupling using a ferrite–palladium-doped BC for the production of bi-aryl compounds under microwave irradiation, achieving a yield of up to 99% using iodine-containing precursors. The authors observed, as in the more traditional systems, a decrease in reactivity using bromide and chloride derivatives.

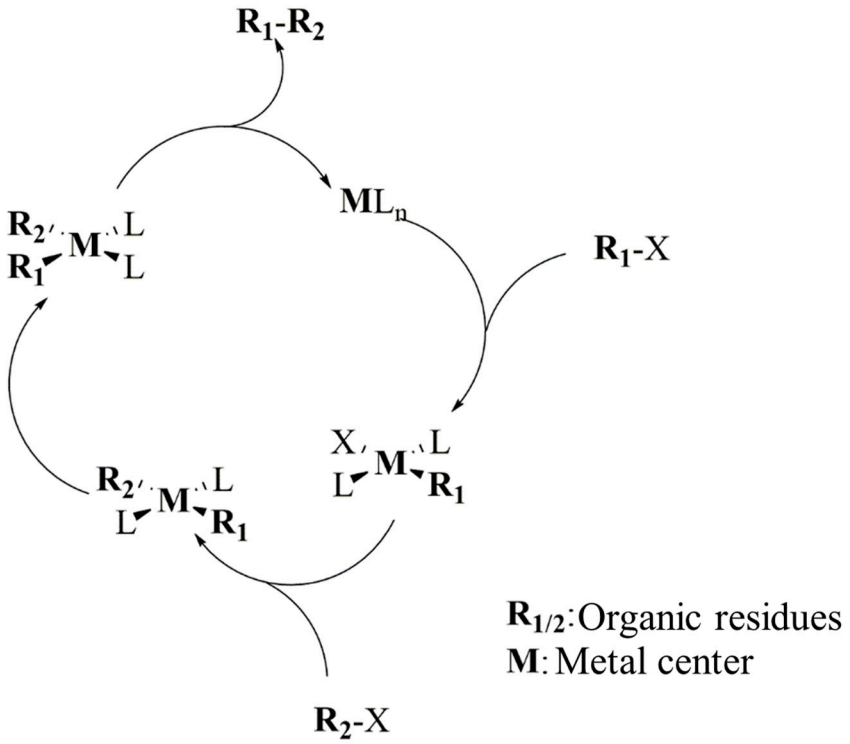

Figure 3. Schematic mechanism of a cross-coupling reaction.

3.1.5. Immobilized Enzyme onto BC

Immobilized enzyme-based catalysts are among the most ground-breaking and game-changing materials in the realm of catalysis. These systems have attracted a great deal of interest from both the industrial and academic worlds [169,170] due to the great specificity, activity, and conversion rate of enzymatic systems, even if their shelf life and operative conditions should still be optimized [170]. The immobilization of enzymes on carbonaceous support is quite common due to the easy chemical functionalization of carbon surfaces [171,172]. The surface functionalization of BC represents an interesting starting point for the production of enzymatic BCSCs for plenty of applications [173].

As reported by Souza Júnior et al. [174], the immobilization procedure adopted matters for the toughness of the enzymatic BCSCs. The authors used the glutaraldehyde conjugation procedure to fix trypsin on activated BC, showing a hydrolytic resistance of over 87% in operative conditions and an increase in activity due to both more efficient feedstock adsorption and a geometrical strain induced by the conjugation. The authors claimed stable catalytic activity for at least four consecutive tests. Similar procedures can be used to immobilize chromate reductase for removing chromium from wastewater operating at 45 °C, reaching a decontamination rate of 98% in a short time [175]. An alternative, glutaraldehyde conjugation, was used to produce peroxidase-based BCSCs to remove phenols [176,177] or to conjugate dehalogenase to remove halo compounds from water solutions [178]. These routes allowed a very efficient treatment of recalcitrant pollutants that can be removed only by using less environmentally sustainable approaches [179,180].

Interestingly, laccases have been found to be very promising in the treatment of such tough waste degradation [181,182]. This enzyme triggers several kinds of reactions by using a complex three-copper active center system [183]. Laccases containing BCSCs have been used to depurate water from plenty of emerging pollutants such as acetaminophen [184], quinolone antibiotics [185], or dyes [186–189]. It was proven that overall system activity can be improved by the alkali-mediated chemical activation of BC support [190].

BC suffers in the confrontation with CNTs and graphene-related materials for the production of enzyme-immobilized materials due to a non-homogenous surface chemistry

compared with carbon allotropes. Nevertheless, BC can be treated as quite homogenous, and the organic tailoring dramatically improves the repeatability of enzyme conjugation procedures.

3.2. Electrochemical Based BC Catalytic Systems

Contrary to thermal catalytic processes, electrocatalytic ones are deeply affected by the quality of the carbon utilized. BC treated at temperatures higher than 800 °C has shown very interesting electric properties [30,191], but they are still far away from those of carbon nanotubes [192] and graphene-related materials [193]. Nevertheless, the electron mobility of thermally annealed BC is quite high [194,195], and the production of self-standing electrodes [196] spread the use of BCSCs in several applications discussed in the next sections.

3.2.1. Electrochemical Oxidation

Electrochemical oxidation is a possible alternative to classical chemical disruption of organic pollutants in watery media with a chemical reaction pathway as represented in Figure 4.

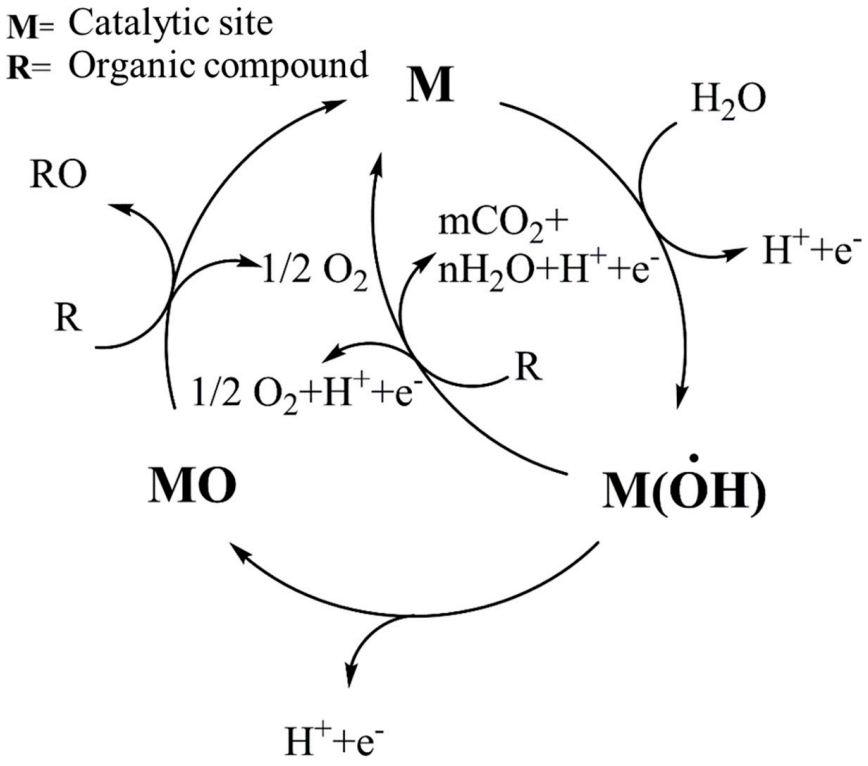

Figure 4. Chemical reactions occurring during electrooxidation of organic compounds.

The mechanism of electro-oxidation involves a metallic active center that is converted into an unstable and very reactive metal hydroxyl radical, promoting the radical degradation of organic species. This approach did not require any oxidant reagents considering that reactive species are produced directly from aqueous medium, but it requires a great deal of energy [197], limiting its applicability to a few scenarios, including the removal of recalcitrant species from wastewater in the civilian [198–203] and pharmaceutical and food [204,205] industries. As an alternative to the mechanism reported in Figure 4, electro-oxidation can proceed through the in situ formation of hydrogen peroxide at the cathode of the system, which acts like an oxidant agent [206]. This is the mechanism exploited by BCSCs, as reported by several authors [176,207–209]. Nevertheless, Dai et al. [210] used BCSCs.

3.2.2. Electrochemical Reduction

Electrochemical reduction is another application of BCSCs of extreme relevance due to the possibility of active removal of carbon dioxide from the gas stream by capturing and converting it through electrochemical devices [211,212]. The mechanism of carbon dioxide reduction is still debatable, but there is consensus that it changes by changing the active material [213–216]. There are a few examples of BCSCs used for the reduction of carbon dioxide using coffee-derived BC as support for bismuth [101] or zinc oxide [217] particles for the production of formic acid or carbon monoxide with high faradic efficiency. In both cases, the BCSCs were prepared through a simple impregnation and calcination process.

3.3. Photochemical Based BC Catalytic Systems

The integration of photocatalytic processes with advanced materials has paved the way for groundbreaking applications in environmental remediation and sustainable technology [218–221]. BCSC photocatalysts stand out as a promising route for harnessing solar energy to drive catalytic reactions [222], as sketched in Figure 5 for ferrite/bismuth oxide supported on biochar for degradation.

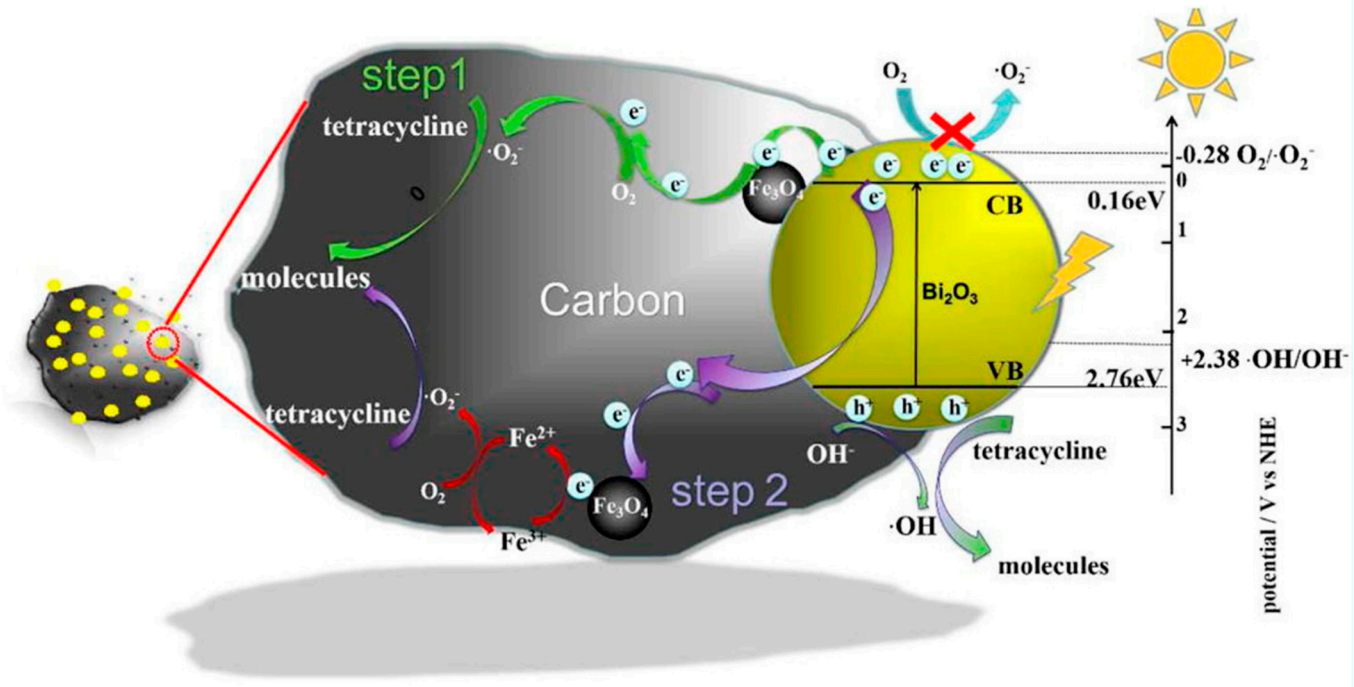

Figure 5. Schematic reactivity of BC photocatalyst as reported by Cui et al. [223]. Picture reprinted with all permission (CC BY-NC-ND 4.0).

Photocatalysts are characterized by their ability to initiate chemical reactions upon light exposure, offering a unique opportunity to address pressing challenges such as water and air pollution, while BC can provide an intriguing platform for hosting and enhancing the performance of these photocatalytic agents. The scientific challenge represented by BCSC photocatalysts delves into the fundamental principles, mechanisms, and potential applications of BC-supported photocatalysts, illuminating a path toward efficient and environmentally friendly solutions to contemporary environmental issues [224]. Accordingly, the majority of the studies about photoactive BCSCs are focused on pollutant degradation and wastewater treatment using well-known materials such as titanium oxide [225–229] or zinc oxide [230,231].

Nevertheless, band-gap tuning is crucial in order to obtain materials that are active under visible light instead of UV. Several authors modified the surface of common titanium oxide by forming heterojunctions between two different phases [232] or by adding metal doping [233–235]. Li et al. [236] rethought the band gap approach by modifying the BC

structure instead of inserting nitrogen defects in order to improve electron mobility and to more efficiently disperse titanium oxide particles. Alternatively, BCSCs active under visible light can be produced by using different metal species such as bismuth oxide [237,238], bismuth oxohalides [239–242], bismuth vanadate [243–245], cadmium sulphide [246], or zinc ferrites [247,248]. Even if the utilization of a carbon-negative cost matrix such as BC, photoactive BCSCs remain out of the range for most on-field applications due to the elevated cost and leaching problem due to the impossibility of tightly anchoring the active species on the carbon matrix through solid bonds.

3.4. BCSCs for Sustainble Energy Sector: A Small Conundrum

The search for renewable and sustainable sources of energy and fuels has driven significant research into innovative catalytic processes [249], together with the development of new set-up and membrane materials [15]. The utilization of BCSCs has found plenty of applications, but the most important for the future of mankind is related to the promotion of a productive paradigm shift towards a more sustainable society. As a clear example, BCSCs offer a compelling platform to enhance the efficiency and specificity of fuel synthesis reactions through bio-oil upgrading, providing a reasonable solution to biofuel production [129,250]. Particularly, BCSCs have been used for tuning the gasification process in order to drive the consolidation of sustainable hydrogen production [251,252]. In the same framework, BCSCs have found several applications as electrode materials for direct carbon fuel cells [253], hydrogen [254,255], methanol [256], and microbial ones [257,258]. Furthermore, BCSCs were also used in the electrolyzers for green hydrogen production [259,260]. Nevertheless, BCSCs failed to reach a ground-breaking effect in these sectors due to their poor competitiveness with traditional oil-based ones. We can confidently state that BC will contribute to reaching the ambitious goal of a negative emission society by supporting the transition to hydrogen-fueled systems [261], but we should also consider that BC is not a solution for everything, especially for the sectors that still require optimization based on sustainability studies.

4. BCSCs Sustainability: A Small Conundrum

The utilization of BC has been discussed intensively by the research community, but there is not a unanimous consensus on its contribution to mitigating environmental impact. The European community has enforced administrative procedures to certify the sustainability of BC [262]. This has become mandatory for the resource-intensive production platforms of BC that require significant amounts of energy and biomass feedstock [263]. In this framework, the choice of feedstock and the pyrolysis unit play a major role. As a matter of fact, the potential land use competition between BC and food production or natural ecosystems is a major concern. Nevertheless, the utilization of biomass waste streams represents an acceptable alternative that reduces the contribution of greenhouse gas emissions due to their combustion while limiting the available feedstock to the waste one. This represents a key reason for searching for relevant industrial applications that could be satisfied by the use under the limitations related to feedstock availability. BCSCs are high-cost materials that represent a perfect application of BC, actively reducing the utilization of carbon produced from the refinery platforms, such as carbon black. Furthermore, the end-life BCSCs can be simply reused as catalysts in the pyrolysis process, enforcing virtuous circular economy principles.

5. Conclusions and Future Perspectives

In this review, we present a brief and schematic picture of the possible use of BCCSs, providing a general overview of the more recent achievements. The simple handability and modifiability of BCSCs have been taken into consideration, considering their low cost compared with carbon black. BCSCs hold significant promise as a sustainable solution for plenty of catalytic processes, but they are not yet up to the mark when the process itself is not fully established, as in the case of the hydrogen sector. Leveraging the unique

properties of BC as a support material can enhance the catalytic activity and stability of BCSCs, and several ways can be exploited based on the circumstances. The balancing of BC feedstock sourcing, tailoring procedures, and waste valorization emerged as key factors for BCSCs to make a disruptive contribution to the creation of a greener and more efficient future. However, the complete realization of the benefits related to BC BCSCs must be balanced with resource availability and the efforts necessary to build a solid, productive infrastructure. Accordingly, we believe that responsible implementation and thoughtful policy development of BC will be key aspects of the realization of a more sustainable and environmentally resilient society.

Author Contributions: Conceptualization, M.B., data curation, M.B., M.G. and A.T.; writing—original draft preparation, M.B., M.G. and A.T.; writing—review and editing, M.B., M.G. and A.T.; visualization, M.B.; supervision, A.T.; project administration, A.T. All authors have read and agreed to the published version of the manuscript.

Funding: This research received no external funding.

Conflicts of Interest: The authors declare no conflict of interest.

References

1. Lindström, B.; Pettersson, L.J. A brief history of catalysis. *Cattech* **2003**, *7*, 130–138. [CrossRef]
2. Armor, J.N. A history of industrial catalysis. *Catal. Today* **2011**, *163*, 3–9. [CrossRef]
3. Lindlar, H. Ein neuer Katalysator für selektive Hydrierungen. *Helv. Chim. Acta* **1952**, *35*, 446–450. [CrossRef]
4. Tamaru, K. On the Action of Carriers in the Catalytic Hydrogenation of Acetylene by Palladium Catalyst. *Bull. Chem. Soc. Jpn.* **1951**, *24*, 177–180. [CrossRef]
5. Adler, S.F.; Keavney, J.J. The physical nature of supported platinum. *J. Phys. Chem.* **1960**, *64*, 208–212. [CrossRef]
6. Yates, D.J.; Sinfelt, J.H. The catalytic activity of rhodium in relation to its state of dispersion. *J. Catal.* **1967**, *8*, 348–358. [CrossRef]
7. Parravano, G. Carbon Monoxide—Steam Reaction on Ruthenium Catalysts. *Ind. Eng. Chem.* **1957**, *49*, 266–271. [CrossRef]
8. Haldeman, R.; Botty, M. On the nature of the carbon deposit of cracking catalysts. *J. Phys. Chem.* **1959**, *63*, 489–496. [CrossRef]
9. Zhu, Y.; Yang, X.; Peng, C.; Priest, C.; Mei, Y.; Wu, G. Carbon-supported single metal site catalysts for electrochemical CO_2 reduction to CO and beyond. *Small* **2021**, *17*, 2005148. [CrossRef]
10. Sui, S.; Wang, X.; Zhou, X.; Su, Y.; Riffat, S.; Liu, C.-J. A comprehensive review of Pt electrocatalysts for the oxygen reduction reaction: Nanostructure, activity, mechanism and carbon support in PEM fuel cells. *J. Mater. Chem. A* **2017**, *5*, 1808–1825. [CrossRef]
11. Jüntgen, H. Activated carbon as catalyst support: A review of new research results. *Fuel* **1986**, *65*, 1436–1446. [CrossRef]
12. Gerber, I.C.; Serp, P. A theory/experience description of support effects in carbon-supported catalysts. *Chem. Rev.* **2019**, *120*, 1250–1349. [CrossRef] [PubMed]
13. Bartoli, M.; Jagdale, P.; Giorcelli, M.; Rovere, M.; Tagliaferro, A. Overview of Nanostructured Carbon-based Catalysts Recent Advances and Perspectives. In *Nanochemistry*; CRC Press: Boca Raton, FL, USA, 2023; pp. 313–338.
14. Su, D.S.; Perathoner, S.; Centi, G. Nanocarbons for the development of advanced catalysts. *Chem. Rev.* **2013**, *113*, 5782–5816. [CrossRef] [PubMed]
15. Altarawneh, R.M.; Pickup, P.G. Determination of the Stoichiometry of Ethanol Oxidation from the Flow Rate Dependence of the Current in a Proton Exchange Membrane Electrolysis Cell. *J. Electrochem. Soc.* **2018**, *165*, F479. [CrossRef]
16. Altarawneh, M.; Alharazneh, G.; Al-Madanat, O. Dielectric properties of single wall carbon nanotubes-based gelatin phantoms. *J. Adv. Dielectr.* **2018**, *8*, 1850010. [CrossRef]
17. Abu Hajleh, M.N.; Al-limoun, M.; Al-Tarawneh, A.; Hijazin, T.J.; Alqaraleh, M.; Khleifat, K.; Al-Madanat, O.Y.; Qaisi, Y.A.; AlSarayreh, A.; Al-Samydai, A. Synergistic Effects of AgNPs and Biochar: A Potential Combination for Combating Lung Cancer and Pathogenic Bacteria. *Molecules* **2023**, *28*, 4757. [CrossRef] [PubMed]
18. Lee, X.J.; Hiew, B.Y.Z.; Lai, K.C.; Lee, L.Y.; Gan, S.; Thangalazhy-Gopakumar, S.; Rigby, S. Review on graphene and its derivatives: Synthesis methods and potential industrial implementation. *J. Taiwan Inst. Chem. Eng.* **2019**, *98*, 163–180. [CrossRef]
19. Quesne, M.G.; Silveri, F.; De Leeuw, N.H.; Catlow, C.R.A. Advances in sustainable catalysis: A computational perspective. *Front. Chem.* **2019**, *7*, 182. [CrossRef]
20. Testa, M.L.; Tummino, M.L. Lignocellulose biomass as a multifunctional tool for sustainable catalysis and chemicals: An overview. *Catalysts* **2021**, *11*, 125. [CrossRef]
21. Bartoli, M.; Arrigo, R.; Malucelli, G.; Tagliaferro, A.; Duraccio, D. Recent Advances in Biochar Polymer Composites. *Polymers* **2022**, *14*, 2506. [CrossRef]
22. Bartoli, M.; Giorcelli, M.; Jagdale, P.; Rovere, M.; Tagliaferro, A. A Review of Non-Soil Biochar Applications. *Materials* **2020**, *13*, 261. [CrossRef] [PubMed]

23. Giorcelli, M.; Bartoli, M. Development of Coffee Biochar Filler for the Production of Electrical Conductive Reinforced Plastic. *Polymers* **2019**, *11*, 17. [CrossRef]
24. Arrigo, R.; Bartoli, M.; Malucelli, G. Poly (lactic Acid)–Biochar Biocomposites: Effect of Processing and Filler Content on Rheological, Thermal, and Mechanical Properties. *Polymers* **2020**, *12*, 892. [CrossRef] [PubMed]
25. Arrigo, R.; Bartoli, M.; Torsello, D.; Ghigo, G.; Malucelli, G. Thermal, dynamic-mechanical and electrical properties of UV-LED curable coatings containing porcupine-like carbon structures. *Mater. Today Commun.* **2021**, *28*, 102630. [CrossRef]
26. Arrigo, R.; Jagdale, P.; Bartoli, M.; Tagliaferro, A.; Malucelli, G. Structure–Property Relationships in Polyethylene-Based Composites Filled with Biochar Derived from Waste Coffee Grounds. *Polymers* **2019**, *11*, 13. [CrossRef] [PubMed]
27. Duraccio, D.; Arrigo, R.; Bartoli, M.; Capra, P.P.; Malucelli, G. Influence of different dry-mixing techniques on the mechanical, thermal, and electrical behavior of ultra-high molecular weight polyethylene/exhausted tire carbon composites. *Polym. Adv. Technol.* **2022**, *33*, 10. [CrossRef]
28. Bartoli, M.; Torsello, D.; Piatti, E.; Giorcelli, M.; Sparavigna, A.C.; Rovere, M.; Ghigo, G.; Tagliaferro, A. Pressure-Responsive Conductive Poly(vinyl alcohol) Composites Containing Waste Cotton Fibers Biochar. *Micromachines* **2022**, *13*, 125. [CrossRef] [PubMed]
29. Torsello, D.; Bartoli, M.; Giorcelli, M.; Rovere, M.; Arrigo, R.; Malucelli, G.; Tagliaferro, A.; Ghigo, G. High Frequency Electromagnetic Shielding by Biochar-Based Composites. *Nanomaterials* **2021**, *11*, 2383. [CrossRef]
30. Torsello, D.; Ghigo, G.; Giorcelli, M.; Bartoli, M.; Rovere, M.; Tagliaferro, A. Tuning the microwave electromagnetic properties of biochar-based composites by annealing. *Carbon Trends* **2021**, *4*, 100062. [CrossRef]
31. Zecchi, S.; Ruscillo, F.; Cristoforo, G.; Bartoli, M.; Loebsack, G.; Kang, K.; Piatti, E.; Torsello, D.; Ghigo, G.; Gerbaldo, R.; et al. Effect of Red Mud Addition on Electrical and Magnetic Properties of Hemp-Derived-Biochar-Containing Epoxy Composites. *Micromachines* **2023**, *14*, 429. [CrossRef]
32. Savi, P.; Yasir, M.; Bartoli, M.; Giorcelli, M.; Longo, M. Electrical and Microwave Characterization of Thermal Annealed Sewage Sludge Derived Biochar Composites. *Appl. Sci.* **2020**, *10*, 1334–1345. [CrossRef]
33. Matta, S.; Bartoli, M.; Arrigo, R.; Frache, A.; Malucelli, G. Flame retardant potential of Tetra Pak®-derived biochar for ethylene-vinyl-acetate copolymers. *Compos. Part C Open Access* **2022**, *8*, 100252. [CrossRef]
34. Matta, S.; Bartoli, M.; Frache, A.; Malucelli, G. Investigation of Different Types of Biochar on the Thermal Stability and Fire Retardance of Ethylene-Vinyl Acetate Copolymers. *Polymers* **2021**, *13*, 1256. [CrossRef] [PubMed]
35. Barbalini, M.; Bartoli, M.; Tagliaferro, A.; Malucelli, G. Phytic Acid and Biochar: An Effective All Bio-Sourced Flame Retardant Formulation for Cotton Fabrics. *Polymers* **2020**, *12*, 811. [CrossRef]
36. Karnati, S.R.; Høgsaa, B.; Zhang, L.; Fini, E.H. Developing carbon nanoparticles with tunable morphology and surface chemistry for use in construction. *Constr. Build. Mater.* **2020**, *262*, 120780. [CrossRef]
37. Bartoli, M.; Rosso, C.; Giorcelli, M.; Rovere, M.; Jagdale, P.; Tagliaferro, A.; Chae, M.; Bressler, D.C. Effect of incorporation of microstructured carbonized cellulose on surface and mechanical properties of epoxy composites. *J. Appl. Polym. Sci.* **2020**, *137*, 48896. [CrossRef]
38. Xie, Y.; Wang, L.; Li, H.; Westholm, L.J.; Carvalho, L.; Thorin, E.; Yu, Z.; Yu, X.; Skreiberg, Ø. A critical review on production, modification and utilization of biochar. *J. Anal. Appl. Pyrolysis* **2022**, *161*, 105405. [CrossRef]
39. Ahmed, M.B.; Zhou, J.L.; Ngo, H.H.; Guo, W. Insight into biochar properties and its cost analysis. *Biomass Bioenergy* **2016**, *84*, 76–86. [CrossRef]
40. Zhu, X.; Labianca, C.; He, M.; Luo, Z.; Wu, C.; You, S.; Tsang, D.C. Life-cycle assessment of pyrolysis processes for sustainable production of biochar from agro-residues. *Bioresour. Technol.* **2022**, *360*, 127601. [CrossRef]
41. Lee, J.; Kim, K.-H.; Kwon, E.E. Biochar as a catalyst. *Renew. Sustain. Energy Rev.* **2017**, *77*, 70–79. [CrossRef]
42. Shan, R.; Han, J.; Gu, J.; Yuan, H.; Luo, B.; Chen, Y. A review of recent developments in catalytic applications of biochar-based materials. *Resour. Conserv. Recycl.* **2020**, *162*, 105036. [CrossRef]
43. Zhou, X.; Zhu, Y.; Niu, Q.; Zeng, G.; Lai, C.; Liu, S.; Huang, D.; Qin, L.; Liu, X.; Li, B. New notion of biochar: A review on the mechanism of biochar applications in advannced oxidation processes. *Chem. Eng. J.* **2021**, *416*, 129027. [CrossRef]
44. Strongone, V.; Bartoli, M.; Jagdale, P.; Arrigo, R.; Tagliaferro, A.; Malucelli, G. Preparation and Characterization of UV-LED Curable Acrylic Films Containing Biochar and/or Multiwalled Carbon Nanotubes: Effect of the Filler Loading on the Rheological, Thermal and Optical Properties. *Polymers* **2020**, *12*, 796. [CrossRef] [PubMed]
45. Maroušek, J.; Vochozka, M.; Plachý, J.; Žák, J. Glory and misery of biochar. *Clean Technol. Environ. Policy* **2017**, *19*, 311–317. [CrossRef]
46. Li, J.; Li, B.; Yu, W.; Huang, H.; Han, J.-C.; Huang, Y.; Wu, X.; Young, B.; Wang, G. Lanthanum-based adsorbents for phosphate reutilization: Interference factors, adsorbent regeneration, and research gaps. *Sustain. Horiz.* **2022**, *1*, 100011. [CrossRef]
47. Huang, Y.; Chen, Y.; Li, X.; Zhu, K.; Jiang, Z.; Yuan, H.; Yan, K. One-step solvothermal construction of coral reef-like FeS_2/biochar to activate peroxymonosulfate for efficient organic pollutant removal. *Sep. Purif. Technol.* **2023**, *308*, 122976. [CrossRef]
48. Li, X.; Hu, K.; Huang, Y.; Gu, Q.; Chen, Y.; Yang, B.; Qiu, R.; Luo, W.; Weckhuysen, B.M.; Yan, K. Upcycling biomass waste into Fe single atom catalysts for pollutant control. *J. Energy Chem.* **2022**, *69*, 282–291. [CrossRef]
49. Zeng, Y.; Zhao, M.; Zeng, H.; Jiang, Q.; Ming, F.; Xi, K.; Wang, Z.; Liang, H. Recent progress in advanced catalysts for electrocatalytic hydrogenation of organics in aqueous conditions. *eScience* **2023**, 100156. [CrossRef]

50. Chen, W.-H.; Peng, J.; Bi, X.T. A state-of-the-art review of biomass torrefaction, densification and applications. *Renew. Sustain. Energy Rev.* **2015**, *44*, 847–866. [CrossRef]
51. Peng, J.; Bi, H.; Lim, C.; Sokhansanj, S. Study on density, hardness, and moisture uptake of torrefied wood pellets. *Energy Fuels* **2013**, *27*, 967–974. [CrossRef]
52. Bridgwater, A.V.; Meier, D.; Radlein, D. An overview of fast pyrolysis of biomass. *Org. Geochem.* **1999**, *30*, 1479–1493. [CrossRef]
53. Huang, Y.; Li, B.; Liu, D.; Xie, X.; Zhang, H.; Sun, H.; Hu, X.; Zhang, S. Fundamental advances in biomass autothermal/oxidative pyrolysis: A review. *ACS Sustain. Chem. Eng.* **2020**, *8*, 11888–11905. [CrossRef]
54. Zeng, K.; Gauthier, D.; Soria, J.; Mazza, G.; Flamant, G. Solar pyrolysis of carbonaceous feedstocks: A review. *Sol. Energy* **2017**, *156*, 73–92. [CrossRef]
55. Huang, Y.-F.; Chiueh, P.-T.; Lo, S.-L. A review on microwave pyrolysis of lignocellulosic biomass. *Sustain. Environ. Res.* **2016**, *26*, 103–109. [CrossRef]
56. Garcia-Nunez, J.; Pelaez-Samaniego, M.; Garcia-Perez, M.; Fonts, I.; Abrego, J.; Westerhof, R.; Garcia-Perez, M. Historical developments of pyrolysis reactors: A review. *Energy Fuels* **2017**, *31*, 5751–5775. [CrossRef]
57. Ni, J.; Qian, L.; Wang, Y.; Zhang, B.; Gu, H.; Hu, Y.; Wang, Q. A review on fast hydrothermal liquefaction of biomass. *Fuel* **2022**, *327*, 125135. [CrossRef]
58. Valizadeh, S.; Hakimian, H.; Farooq, A.; Jeon, B.-H.; Chen, W.-H.; Lee, S.H.; Jung, S.-C.; Seo, M.W.; Park, Y.-K. Valorization of biomass through gasification for green hydrogen generation: A comprehensive review. *Bioresour. Technol.* **2022**, *365*, 128143. [CrossRef] [PubMed]
59. Downie, A.; Crosky, A.; Munroe, P. Physical properties of biochar. In *Biochar for Environmental Management*, 1st ed.; Routledge: Abingdon, UK, 2009.
60. Tagliaferro, A.; Rovere, M.; Padovano, E.; Bartoli, M.; Giorcelli, M. Introducing the Novel Mixed Gaussian-Lorentzian Lineshape in the Analysis of the Raman Signal of Biochar. *Nanomaterials* **2020**, *10*, 1748. [CrossRef]
61. Franklin, R.E. Crystallite growth in graphitizing and non-graphitizing carbons. *Proc. R. Soc. Lond. Ser. A Math. Phys. Sci.* **1951**, *209*, 196–218.
62. Weber, K.; Quicker, P. Properties of biochar. *Fuel* **2018**, *217*, 240–261. [CrossRef]
63. Bartoli, M.; Troiano, M.; Giudicianni, P.; Amato, D.; Giorcelli, M.; Solimene, R.; Tagliaferro, A. Effect of heating rate and feedstock nature on electrical conductivity of biochar and biochar-based composites. *Appl. Energy Combust. Sci.* **2022**, *12*, 100089. [CrossRef]
64. Oberlin, A. *High-Resolution TEM Studies of Carbonization and Graphitization*; Thrower, P.A., Ed.; Marcel Dekker Inc.: New York, NY, USA, 1989; Volume 22.
65. Edstrom, T.; Lewis, I. Chemical structure and graphitization: X-ray diffraction studies of graphites derived from polynuclear aromatics. *Carbon* **1969**, *7*, 85–91. [CrossRef]
66. Liu, W.-J.; Jiang, H.; Yu, H.-Q. Emerging applications of biochar-based materials for energy storage and conversion. *Energy Environ. Sci.* **2019**, *12*, 1751–1779. [CrossRef]
67. Cheng, B.-H.; Zeng, R.J.; Jiang, H. Recent developments of post-modification of biochar for electrochemical energy storage. *Bioresour. Technol.* **2017**, *246*, 224–233. [CrossRef] [PubMed]
68. Scott, S.L.; Crudden, C.M.; Jones, C.W. *Nanostructured Catalysts*; Springer Science & Business Media: Chicago, IL, USA, 2008.
69. Burakov, A.E.; Galunin, E.V.; Burakova, I.V.; Kucherova, A.E.; Agarwal, S.; Tkachev, A.G.; Gupta, V.K. Adsorption of heavy metals on conventional and nanostructured materials for wastewater treatment purposes: A review. *Ecotoxicol. Environ. Saf.* **2018**, *148*, 702–712. [CrossRef] [PubMed]
70. Di Noto, V.; Negro, E.; Patil, B.; Lorandi, F.; Boudjelida, S.; Bang, Y.H.; Vezzù, K.; Pagot, G.; Crociani, L.; Nale, A. Hierarchical Metal-[Carbon Nitride Shell/Carbon Core] Electrocatalysts: A Promising New General Approach to Tackle the ORR Bottleneck in Low-Temperature Fuel Cells. *ACS Catal.* **2022**, *12*, 12291–12301. [CrossRef]
71. Lei, H.; Li, J.; Zhang, X.; Ma, L.; Ji, Z.; Wang, Z.; Pan, L.; Tan, S.; Mai, W. A review of hard carbon anode: Rational design and advanced characterization in potassium ion batteries. *InfoMat* **2022**, *4*, e12272. [CrossRef]
72. Serp, P.; Figueiredo, J.L. *Carbon Materials for Catalysis*; Wiley: Hoboken, NJ, USA, 2008; pp. 1–579.
73. Nisticò, R.; Guerretta, F.; Benzi, P.; Magnacca, G. Chitosan-derived biochars obtained at low pyrolysis temperatures for potential application in electrochemical energy storage devices. *Int. J. Biol. Macromol.* **2020**, *164*, 1825–1831. [CrossRef]
74. Xu, X.; Zheng, Y.; Gao, B.; Cao, X. N-doped biochar synthesized by a facile ball-milling method for enhanced sorption of CO_2 and reactive red. *Chem. Eng. J.* **2019**, *368*, 564–572. [CrossRef]
75. Wang, X.; Liu, Y.; Zhu, L.; Li, Y.; Wang, K.; Qiu, K.; Tippayawong, N.; Aggarangsi, P.; Reubroycharoen, P.; Wang, S. Biomass derived N-doped biochar as efficient catalyst supports for CO_2 methanation. *J. CO_2 Util.* **2019**, *34*, 733–741. [CrossRef]
76. Suo, F.; You, X.; Ma, Y.; Li, Y. Rapid removal of triazine pesticides by P doped biochar and the adsorption mechanism. *Chemosphere* **2019**, *235*, 918–925. [CrossRef]
77. Cheah, S.; Malone, S.C.; Feik, C.J. Speciation of Sulfur in Biochar Produced from Pyrolysis and Gasification of Oak and Corn Stover. *Environ. Sci. Technol.* **2014**, *48*, 8474–8480. [CrossRef] [PubMed]
78. Leng, L.; Liu, R.; Xu, S.; Mohamed, B.A.; Yang, Z.; Hu, Y.; Chen, J.; Zhao, S.; Wu, Z.; Peng, H.; et al. An overview of sulfur-functional groups in biochar from pyrolysis of biomass. *J. Environ. Chem. Eng.* **2022**, *10*, 107185. [CrossRef]
79. O'Connor, D.; Peng, T.; Li, G.; Wang, S.; Duan, L.; Mulder, J.; Cornelissen, G.; Cheng, Z.; Yang, S.; Hou, D. Sulfur-modified rice husk biochar: A green method for the remediation of mercury contaminated soil. *Sci. Total Environ.* **2018**, *621*, 819–826. [CrossRef]

80. Sui, L.; Tang, C.; Du, Q.; Zhao, Y.; Cheng, K.; Yang, F. Preparation and characterization of boron-doped corn straw biochar: Fe (II) removal equilibrium and kinetics. *J. Environ. Sci.* **2021**, *106*, 116–123. [CrossRef] [PubMed]
81. Yao, Q.; Borjihan, Q.; Qu, H.; Guo, Y.; Zhao, Z.; Qiao, L.; Li, T.; Dong, A.; Liu, Y. Cow dung-derived biochars engineered as antibacterial agents for bacterial decontamination. *J. Environ. Sci.* **2021**, *105*, 33–43. [CrossRef] [PubMed]
82. Bamdad, H.; Hawboldt, K. Comparative study between physicochemical characterization of biochar and metal organic frameworks (MOFs) as gas adsorbents. *Can. J. Chem. Eng.* **2016**, *94*, 2114–2120. [CrossRef]
83. Azargohar, R.; Dalai, A. Steam and KOH activation of biochar: Experimental and modeling studies. *Microporous Mesoporous Mater.* **2008**, *110*, 413–421. [CrossRef]
84. Lee, H.W.; Kim, Y.-M.; Kim, S.; Ryu, C.; Park, S.H.; Park, Y.-K. Review of the use of activated biochar for energy and environmental applications. *Carbon Lett.* **2018**, *26*, 1–10.
85. Bouchelta, C.; Medjram, M.S.; Bertrand, O.; Bellat, J.-P. Preparation and characterization of activated carbon from date stones by physical activation with steam. *J. Anal. Appl. Pyrolysis* **2008**, *82*, 70–77. [CrossRef]
86. Heidarinejad, Z.; Dehghani, M.H.; Heidari, M.; Javedan, G.; Ali, I.; Sillanpää, M. Methods for preparation and activation of activated carbon: A review. *Environ. Chem. Lett.* **2020**, *18*, 393–415. [CrossRef]
87. Moreno-Castilla, C.; Ferro-Garcia, M.; Joly, J.; Bautista-Toledo, I.; Carrasco-Marin, F.; Rivera-Utrilla, J. Activated carbon surface modifications by nitric acid, hydrogen peroxide, and ammonium peroxydisulfate treatments. *Langmuir* **1995**, *11*, 4386–4392. [CrossRef]
88. Oginni, O.; Singh, K.; Oporto, G.; Dawson-Andoh, B.; McDonald, L.; Sabolsky, E. Effect of one-step and two-step H3PO4 activation on activated carbon characteristics. *Bioresour. Technol. Rep.* **2019**, *8*, 100307. [CrossRef]
89. Acemioğlu, B. Removal of a reactive dye using NaOH-activated biochar prepared from peanut shell by pyrolysis process. *Int. J. Coal Prep. Util.* **2019**, *42*, 671–693. [CrossRef]
90. Han, X.; Chu, L.; Liu, S.; Chen, T.; Ding, C.; Yan, J.; Cui, L.; Quan, G. Removal of methylene blue from aqueous solution using porous biochar obtained by KOH activation of peanut shell biochar. *BioResources* **2015**, *10*, 2836–2849. [CrossRef]
91. Uçar, S.; Erdem, M.; Tay, T.; Karagöz, S. Removal of lead (II) and nickel (II) ions from aqueous solution using activated carbon prepared from rapeseed oil cake by Na2CO3 activation. *Clean Technol. Environ. Policy* **2015**, *17*, 747–756. [CrossRef]
92. Wang, L.; Sun, F.; Hao, F.; Qu, Z.; Gao, J.; Liu, M.; Wang, K.; Zhao, G.; Qin, Y. A green trace K2CO3 induced catalytic activation strategy for developing coal-converted activated carbon as advanced candidate for CO_2 adsorption and supercapacitors. *Chem. Eng. J.* **2020**, *383*, 123205. [CrossRef]
93. Huang, D.; Wang, Y.; Zhang, C.; Zeng, G.; Lai, C.; Wan, J.; Qin, L.; Zeng, Y. Influence of morphological and chemical features of biochar on hydrogen peroxide activation: Implications on sulfamethazine degradation. *RSC Adv.* **2016**, *6*, 73186–73196. [CrossRef]
94. Huang, B.-C.; Jiang, J.; Huang, G.-X.; Yu, H.-Q. Sludge biochar-based catalysts for improved pollutant degradation by activating peroxymonosulfate. *J. Mater. Chem. A* **2018**, *6*, 8978–8985. [CrossRef]
95. Grilla, E.; Vakros, J.; Konstantinou, I.; Manariotis, I.D.; Mantzavinos, D. Activation of persulfate by biochar from spent malt rootlets for the degradation of trimethoprim in the presence of inorganic ions. *J. Chem. Technol. Biotechnol.* **2020**, *95*, 2348–2358. [CrossRef]
96. Zhang, J.; Tahmasebi, A.; Omoriyekomwan, J.E.; Yu, J. Production of carbon nanotubes on bio-char at low temperature via microwave-assisted CVD using Ni catalyst. *Diam. Relat. Mater.* **2019**, *91*, 98–106. [CrossRef]
97. Bartoli, M.; Giorcelli, M.; Rovere, M.; Jagdale, P.; Tagliaferro, A.; Chae, M.; Bressler, D.C. Shape tunability of carbonized cellulose nanocrystals. *SN Appl. Sci.* **2019**, *1*, 1661–1676. [CrossRef]
98. Folarin, O.M.; Sadiku, E.R.; Maity, A. Polymer-noble metal nanocomposites. *Int. J. Phys. Sci.* **2011**, *6*, 4869–4882.
99. Dobrzański, L.; Pawlyta, M.; Krztoń, A.; Liszka, B.; Labisz, K. Synthesis and characterization of carbon nanotubes decorated with platinum nanoparticles. *J. Achiev. Mater. Manuf. Eng.* **2010**, *39*, 184–189.
100. Kuzminykh, Y.; Dabirian, A.; Reinke, M.; Hoffmann, P. High vacuum chemical vapour deposition of oxides: A review of technique development and precursor selection. *Surf. Coat. Technol.* **2013**, *230*, 13–21. [CrossRef]
101. Zeng, J.; Jagdale, P.; Lourenço, M.A.O.; Farkhondehfal, M.A.; Sassone, D.; Bartoli, M.; Pirri, C.F. Biochar-Supported BiOx for Effective Electrosynthesis of Formic Acid from Carbon Dioxide Reduction. *Crystals* **2021**, *11*, 363. [CrossRef]
102. Shen, Y. Carbothermal synthesis of metal-functionalized nanostructures for energy and environmental applications. *J. Mater. Chem. A* **2015**, *3*, 13114–13188. [CrossRef]
103. Tamborrino, V.; Costamagna, G.; Bartoli, M.; Rovere, M.; Jagdale, P.; Lavagna, L.; Ginepro, M.; Tagliaferro, A. Catalytic oxidative desulphurization of pyrolytic oils to fuels over different waste derived carbon-based catalysts. *Fuel* **2021**, *296*, 120693. [CrossRef]
104. Piatti, E.; Torsello, D.; Gavello, G.; Ghigo, G.; Gerbaldo, R.; Bartoli, M.; Duraccio, D. Tailoring the Magnetic and Electrical Properties of Epoxy Composites Containing Olive-Derived Biochar through Iron Modification. *Nanomaterials* **2023**, *13*, 2326. [CrossRef]
105. Ippolito, J.A.; Cui, L.; Kammann, C.; Wrage-Mönnig, N.; Estavillo, J.M.; Fuertes-Mendizabal, T.; Cayuela, M.L.; Sigua, G.; Novak, J.; Spokas, K. Feedstock choice, pyrolysis temperature and type influence biochar characteristics: A comprehensive meta-data analysis review. *Biochar* **2020**, *2*, 421–438. [CrossRef]
106. Tomczyk, A.; Sokołowska, Z.; Boguta, P. Biochar physicochemical properties: Pyrolysis temperature and feedstock kind effects. *Rev. Environ. Sci. Bio/Technol.* **2020**, *19*, 191–215. [CrossRef]

107. Liu, Y.; Chen, Y.; Li, Y.; Chen, L.; Jiang, H.; Li, H.; Luo, X.; Tang, P.; Yan, H.; Zhao, M. Fabrication, application, and mechanism of metal and heteroatom co-doped biochar composites (MHBCs) for the removal of contaminants in water: A review. *J. Hazard. Mater.* **2022**, *431*, 128584. [CrossRef] [PubMed]
108. Panwar, N.; Pawar, A. Influence of activation conditions on the physicochemical properties of activated biochar: A review. *Biomass Convers. Biorefin.* **2020**, *12*, 925–947. [CrossRef]
109. Patel, A.K.; Singhania, R.R.; Pal, A.; Chen, C.-W.; Pandey, A.; Dong, C.-D. Advances on tailored biochar for bioremediation of antibiotics, pesticides and polycyclic aromatic hydrocarbon pollutants from aqueous and solid phases. *Sci. Total Environ.* **2022**, *817*, 153054. [CrossRef] [PubMed]
110. Qu, J.; Shi, J.; Wang, Y.; Tong, H.; Zhu, Y.; Xu, L.; Wang, Y.; Zhang, B.; Tao, Y.; Dai, X. Applications of functionalized magnetic biochar in environmental remediation: A review. *J. Hazard. Mater.* **2022**, *434*, 128841. [CrossRef] [PubMed]
111. Santos, J.L.; Sanz-Moral, L.M.; Aho, A.; Ivanova, S.; Murzin, D.Y.; Centeno, M.A. Structure effect of modified biochar in Ru/C catalysts for sugar mixture hydrogenation. *Biomass Bioenergy* **2022**, *163*, 106504. [CrossRef]
112. Qin, Y.; Shi, J.; Bai, X. Preparing ultra-stable Ru nanocatalysts supported on partially graphitized biochar via carbothermal reduction for hydrogen storage of N-ethylcarbazole. *Int. J. Hydrogen Energy* **2021**, *46*, 25543–25554. [CrossRef]
113. Sadjadi, S.; Akbari, M.; Léger, B.; Monflier, E.; Heravi, M.M. Eggplant-Derived Biochar-Halloysite Nanocomposite as Supports of Pd Nanoparticles for the Catalytic Hydrogenation of Nitroarenes in the Presence of Cyclodextrin. *ACS Sustain. Chem. Eng.* **2019**, *7*, 6720–6731. [CrossRef]
114. Wang, Y.; Shao, Y.; Zhang, L.; Zhang, S.; Wang, Y.; Xiang, J.; Hu, S.; Hu, G.; Hu, X. Co-presence of hydrophilic and hydrophobic sites in Ni/biochar catalyst for enhancing the hydrogenation activity. *Fuel* **2021**, *293*, 120426. [CrossRef]
115. Dou, M.; Qiao, Y.; Hu, X.; Miao, H.; Zhou, L.; Li, X.; Hou, X.; Wang, Y.; Tang, M. Gradient porous biochar materials with high specific surface area as supports for Pd/C catalysts for efficient maleic acid hydrogenation. *Mol. Catal.* **2023**, *545*, 113218. [CrossRef]
116. Kumar, A.; Kumar, J.; Bhaskar, T. High surface area biochar from Sargassum tenerrimum as potential catalyst support for selective phenol hydrogenation. *Environ. Res.* **2020**, *186*, 109533. [CrossRef] [PubMed]
117. Marques, I.S.; Jarrais, B.; Ramos, R.; Abdelkader-Fernandez, V.K.; Yaremchenko, A.; Freire, C.; Fernandes, D.M.; Peixoto, A.F. Nitrogen-doped biochar-supported metal catalysts: High efficiency in both catalytic transfer hydrogenation of furfural and electrocatalytic oxygen reactions. *Catal. Today* **2023**, *418*, 114080. [CrossRef]
118. Ren, X.; Tang, L.; Wang, J.; Almatrafi, E.; Feng, H.; Tang, X.; Yu, J.; Yang, Y.; Li, X.; Zhou, C.; et al. Highly efficient catalytic hydrogenation of nitrophenols by sewage sludge derived biochar. *Water Res.* **2021**, *201*, 117360. [CrossRef] [PubMed]
119. Fu, Q.; Xu, X.; Miao, R.; Wang, M.; Zhou, H.; He, L.; Guan, Q. Mn-embedded porous rubber seed shell biochar for enhanced removal of copper ions and catalytic efficacy of the used adsorbent for hydrogenation of furfural. *Chem. Eng. J.* **2022**, *441*, 136065. [CrossRef]
120. Wang, Y.-Y.; Ling, L.-L.; Jiang, H. Selective hydrogenation of lignin to produce chemical commodities by using a biochar supported Ni–Mo 2 C catalyst obtained from biomass. *Green Chem.* **2016**, *18*, 4032–4041. [CrossRef]
121. Yang, X.; Shao, S.; Li, X.; Tang, D. Catalytic transfer hydrogenation of bio-oil over biochar-based CuO catalyst using methanol as hydrogen donor. *Renew. Energy* **2023**, *211*, 21–30. [CrossRef]
122. Zou, R.; Wang, C.; Qian, M.; Huo, E.; Kong, X.; Wang, Y.; Dai, L.; Wang, L.; Zhang, X.; Mateo, W.C.; et al. Catalytic co-pyrolysis of solid wastes (low-density polyethylene and lignocellulosic biomass) over microwave assisted biochar for bio-oil upgrading and hydrogen production. *J. Clean. Prod.* **2022**, *374*, 133971. [CrossRef]
123. Van den Bosch, S.; Schutyser, W.; Koelewijn, S.-F.; Renders, T.; Courtin, C.; Sels, B. Tuning the lignin oil OH-content with Ru and Pd catalysts during lignin hydrogenolysis on birch wood. *Chem. Commun.* **2015**, *51*, 13158–13161. [CrossRef]
124. Shen, Y.; Yoshikawa, K. Tar conversion and vapor upgrading via in situ catalysis using silica-based nickel nanoparticles embedded in rice husk char for biomass pyrolysis/gasification. *Ind. Eng. Chem. Res.* **2014**, *53*, 10929–10942. [CrossRef]
125. Lin, Y.-C.; Li, C.-L.; Wan, H.-P.; Lee, H.-T.; Liu, C.-F. Catalytic hydrodeoxygenation of guaiacol on Rh-based and sulfided CoMo and NiMo catalysts. *Energy Fuels* **2011**, *25*, 890–896. [CrossRef]
126. Gupta, S.; Mondal, P.; Borugadda, V.B.; Dalai, A.K. Advances in upgradation of pyrolysis bio-oil and biochar towards improvement in bio-refinery economics: A comprehensive review. *Environ. Technol. Innov.* **2021**, *21*, 101276. [CrossRef]
127. Bartoli, M.; Rosi, L.; Frediani, P.; Frediani, M. Bio-oils from microwave assisted pyrolysis of kraft lignin operating at reduced residual pressure. *Fuel* **2020**, *278*, 118175. [CrossRef]
128. Bridgwater, A. 7—Fast pyrolysis of biomass for the production of liquids. In *Biomass Combustion Science, Technology and Engineering*; Rosendahl, L., Ed.; Woodhead Publishing: Sawston, UK, 2013; pp. 130–171.
129. Qiu, Z.; Zhai, Y.; Li, S.; Liu, X.; Liu, X.; Wang, B.; Liu, Y.; Li, C.; Hu, Y. Catalytic co-pyrolysis of sewage sludge and rice husk over biochar catalyst: Bio-oil upgrading and catalytic mechanism. *Waste Manag.* **2020**, *114*, 225–233. [CrossRef]
130. Liu, S.; Wu, G.; Gao, Y.; Li, B.; Feng, Y.; Zhou, J.; Hu, X.; Huang, Y.; Zhang, S.; Zhang, H. Understanding the catalytic upgrading of bio-oil from pine pyrolysis over CO_2-activated biochar. *Renew. Energy* **2021**, *174*, 538–546. [CrossRef]
131. Jiang, T.; Wang, B.; Gao, B.; Cheng, N.; Feng, Q.; Chen, M.; Wang, S. Degradation of organic pollutants from water by biochar-assisted advanced oxidation processes: Mechanisms and applications. *J. Hazard. Mater.* **2023**, *442*, 130075. [CrossRef] [PubMed]
132. Bartoli, M.; Zhu, C.; Asomaning, J.; Chae, M.; Bressler, D.C. Biosolids-based catalyst for oxidative desulphurization of drop-in fuels derived from waste fats. *Fuel* **2022**, *324*, 124546. [CrossRef]

133. Pignatello, J.J.; Oliveros, E.; MacKay, A. Advanced oxidation processes for organic contaminant destruction based on the Fenton reaction and related chemistry. *Crit. Rev. Environ. Sci. Technol.* **2006**, *36*, 1–84. [CrossRef]
134. Barb, W.G.; Baxendale, J.H.; George, P.; Hargrave, K.R. Reactions of ferrous and ferric ions with hydrogen peroxide. Part I—The ferrous ion reaction. *Trans. Farady Soc.* **1951**, *47*, 462–500. [CrossRef]
135. Barb, W.G.; Baxendale, J.H.; George, P.; Hargrave, K.R. Reactions of ferrous and ferric ions with hydrogen peroxide. Part II—The ferric ion reaction. *Trans. Faraday Soc.* **1951**, *47*, 591–616. [CrossRef]
136. Ensing, B.; Buda, F.; Baerends, E.J. Fenton-like chemistry in water: Oxidation catalysis by Fe (III) and H_2O_2. *J. Phys. Chem. A* **2003**, *107*, 5722–5731. [CrossRef]
137. Koppenol, W. The centennial of the Fenton reaction. *Free Radic. Biol. Med.* **1993**, *15*, 645–651. [CrossRef] [PubMed]
138. Thomas, N.; Dionysiou, D.D.; Pillai, S.C. Heterogeneous Fenton catalysts: A review of recent advances. *J. Hazard. Mater.* **2021**, *404*, 124082. [CrossRef] [PubMed]
139. Manjuri Bhuyan, P.; Borah, S.; Kumar Bhuyan, B.; Hazarika, S.; Gogoi, N.; Gogoi, A.; Gogoi, P. Fe3S4/biochar catalysed heterogeneous Fenton oxidation of organic contaminants: Hydrogen peroxide activation and biochar enhanced reduction of Fe (III) to Fe (II). *Sep. Purif. Technol.* **2023**, *312*, 123387. [CrossRef]
140. Devi, P.; Dalai, A.K.; Chaurasia, S.P. Activity and stability of biochar in hydrogen peroxide based oxidation system for degradation of naphthenic acid. *Chemosphere* **2020**, *241*, 125007. [CrossRef] [PubMed]
141. Wang, Y.; Dong, H.; Li, L.; Tian, R.; Chen, J.; Ning, Q.; Wang, B.; Tang, L.; Zeng, G. Influence of feedstocks and modification methods on biochar's capacity to activate hydrogen peroxide for tetracycline removal. *Bioresour. Technol.* **2019**, *291*, 121840. [CrossRef] [PubMed]
142. Yang, J.; Li, Y.; Yang, Z.; Ying, G.-G.; Shih, K.; Feng, Y. Hydrogen peroxide as a key intermediate for hydroxyl radical generation during catalytic ozonation of biochar: Mechanistic insights into the evolution and contribution of radicals. *Sep. Purif. Technol.* **2023**, *324*, 124525. [CrossRef]
143. Tao, S.; Liang, S.; Chen, Y.; Yu, W.; Hou, H.; Qiu, J.; Zhu, Y.; Xiao, K.; Hu, J.; Liu, B.; et al. Enhanced sludge dewaterability with sludge-derived biochar activating hydrogen peroxide: Synergism of Fe and Al elements in biochar. *Water Res.* **2020**, *182*, 115927. [CrossRef] [PubMed]
144. Xing, L.; Wei, J.; Zhang, Y.; Xu, M.; Pan, G.; Li, J.; Li, J.; Li, Y. Boosting active sites of protogenetic sludge-based biochar by boron doping for electro-Fenton degradation towards emerging organic contaminants. *Sep. Purif. Technol.* **2022**, *294*, 121160. [CrossRef]
145. Li, H.; Dai, T.; Chen, J.; Chen, L.; Li, Y.; Kan, X.; Hou, H.; Han, Y. Enhanced sludge dewaterability by Fe-rich biochar activating hydrogen peroxide: Co-hydrothermal red mud and reed straw. *J. Environ. Manag.* **2021**, *296*, 113239. [CrossRef]
146. Li, L.; Cheng, M.; Qin, L.; Almatrafi, E.; Yang, X.; Yang, L.; Tang, C.; Liu, S.; Yi, H.; Zhang, M.; et al. Enhancing hydrogen peroxide activation of CuCo layered double hydroxide by compositing with biochar: Performance and mechanism. *Sci. Total Environ.* **2022**, *828*, 154188. [CrossRef]
147. Chen, Q.; Cheng, Z.; Li, X.; Wang, C.; Yan, L.; Shen, G.; Shen, Z. Degradation mechanism and QSAR models of antibiotic contaminants in soil by MgFe-LDH engineered biochar activating urea-hydrogen peroxide. *Appl. Catal. B Environ.* **2022**, *302*, 120866. [CrossRef]
148. Cheng, Z.; Chen, Q.; Liu, S.; Liu, Y.; Ren, Y.; Zhang, X.; Shen, Z. The investigation of influencing factors on the degradation of sulfonamide antibiotics in iron-impregnated biochar-activated urea-hydrogen peroxide system: A QSAR study. *J. Hazard. Mater.* **2022**, *430*, 128269. [CrossRef] [PubMed]
149. Bartoli, M.; Asomaning, J.; Xia, L.; Chae, M.; Bressler, D.C. Desulphurization of drop-in fuel produced through lipid pyrolysis using brown grease and biosolids feedstocks. *Biomass Bioenergy* **2021**, *154*, 106233. [CrossRef]
150. Yuan, Y.; Huang, L.; Yılmaz, M.; Zhang, T.C.; Wang, Y.; Yuan, S. $MgFe_2O_4$-loaded N-doped biochar derived from waste cooked rice for efficient low-temperature desulfurization of H_2S. *Fuel* **2023**, *339*, 127385. [CrossRef]
151. Yuan, Y.; Huang, L.; Zhang, T.C.; Wang, Y.; Yuan, S. $CaCO_3$-ZnO loaded scrap rice-derived biochar for H2S removal at room-temperature: Characterization, performance and mechanism. *Fuel Process. Technol.* **2023**, *249*, 107846. [CrossRef]
152. Tan, X.; Zhang, C.; Wei, H.; Shi, P.; Chang, H.; Ho, S.-H. Versatile strategy of sulfanilamide antibiotics removal via microalgal biochar: Role of oxygen-enriched functional groups. *Chemosphere* **2022**, *304*, 135244. [CrossRef] [PubMed]
153. Wu, D.; Chen, Q.; Wu, M.; Zhang, P.; He, L.; Chen, Y.; Pan, B. Heterogeneous compositions of oxygen-containing functional groups on biochars and their different roles in rhodamine B degradation. *Chemosphere* **2022**, *292*, 133518. [CrossRef]
154. Qi, Z.; Chen, L.; Zhang, S.; Su, J.; Somorjai, G.A. A mini review of cobalt-based nanocatalyst in Fischer-Tropsch synthesis. *Appl. Catal. A Gen.* **2020**, *602*, 117701. [CrossRef]
155. Jahangiri, H.; Bennett, J.; Mahjoubi, P.; Wilson, K.; Gu, S. A review of advanced catalyst development for Fischer–Tropsch synthesis of hydrocarbons from biomass derived syn-gas. *Catal. Sci. Technol.* **2014**, *4*, 2210–2229. [CrossRef]
156. Ma, W.; Jacobs, G.; Sparks, D.E.; Todic, B.; Bukur, D.B.; Davis, B.H. Quantitative comparison of iron and cobalt based catalysts for the Fischer-Tropsch synthesis under clean and poisoning conditions. *Catal. Today* **2020**, *343*, 125–136. [CrossRef]
157. Sun, B.; Xu, K.; Nguyen, L.; Qiao, M.; Tao, F. Preparation and catalysis of carbon-supported iron catalysts for Fischer–Tropsch synthesis. *ChemCatChem* **2012**, *4*, 1498–1511. [CrossRef]
158. Oschatz, M.; Krans, N.; Xie, J.; de Jong, K.P. Systematic variation of the sodium/sulfur promoter content on carbon-supported iron catalysts for the Fischer–Tropsch to olefins reaction. *J. Energy Chem.* **2016**, *25*, 985–993. [CrossRef]

159. Yousefian, F.; Babatabar, M.A.; Eshaghi, M.; Poor, S.M.; Tavasoli, A. Pyrolysis of Rice husk, Coconut shell, and Cladophora glomerata algae and application of the produced biochars as support for cobalt catalyst in Fischer–Tropsch synthesis. *Fuel Process. Technol.* **2023**, *247*, 107818. [CrossRef]
160. Yan, Q.; Wan, C.; Liu, J.; Gao, J.; Yu, F.; Zhang, J.; Cai, Z. Iron nanoparticles in situ encapsulated in biochar-based carbon as an effective catalyst for the conversion of biomass-derived syngas to liquid hydrocarbons. *Green Chem.* **2013**, *15*, 1631–1640. [CrossRef]
161. Teimouri, Z.; Abatzoglou, N.; Dalai, A.K. Design of a renewable catalyst support derived from biomass with optimized textural features for fischer tropsch synthesis. *Renew. Energy* **2023**, *202*, 1096–1109. [CrossRef]
162. Bai, J.; Qin, C.; Xu, Y.; Xu, D.; Ding, M. Preparation of Nitrogen Doped Biochar-Based Iron Catalyst for Enhancing Gasoline-Range Hydrocarbons Production. *ACS Appl. Mater. Interfaces* **2022**, *14*, 45516–45525. [CrossRef] [PubMed]
163. Corbet, J.-P.; Mignani, G. Selected patented cross-coupling reaction technologies. *Chem. Rev.* **2006**, *106*, 2651–2710. [CrossRef]
164. Miyaura, N.; Buchwald, S.L. *Cross-Coupling Reactions: A Practical Guide*; Springer: Berlin/Heidelberg, Germany, 2002; Volume 219.
165. Negishi, E.-I. A genealogy of Pd-catalyzed cross-coupling. *J. Organomet. Chem.* **2002**, *653*, 34–40. [CrossRef]
166. Pagliaro, M.; Pandarus, V.; Ciriminna, R.; Béland, F.; Demma Carà, P. Heterogeneous versus Homogeneous Palladium Catalysts for Cross-Coupling Reactions. *ChemCatChem* **2012**, *4*, 432–445. [CrossRef]
167. Cornelio, B.; Rance, G.A.; Laronze-Cochard, M.; Fontana, A.; Sapi, J.; Khlobystov, A.N. Palladium nanoparticles on carbon nanotubes as catalysts of cross-coupling reactions. *J. Mater. Chem. A* **2013**, *1*, 8737–8744. [CrossRef]
168. Akay, S.; Baran, T.; Kayan, B.; Kalderis, D. Assessment of a Pd–Fe_3O_4-biochar nanocomposite as a heterogeneous catalyst for the solvent-free Suzuki-Miyaura reaction. *Mater. Chem. Phys.* **2021**, *259*, 124176. [CrossRef]
169. DiCosimo, R.; McAuliffe, J.; Poulose, A.J.; Bohlmann, G. Industrial use of immobilized enzymes. *Chem. Soc. Rev.* **2013**, *42*, 6437–6474. [CrossRef] [PubMed]
170. Ansari, S.A.; Husain, Q. Potential applications of enzymes immobilized on/in nano materials: A review. *Biotechnol. Adv.* **2012**, *30*, 512–523. [CrossRef] [PubMed]
171. Zhang, J.; Zhang, F.; Yang, H.; Huang, X.; Liu, H.; Zhang, J.; Guo, S. Graphene oxide as a matrix for enzyme immobilization. *Langmuir* **2010**, *26*, 6083–6085. [CrossRef] [PubMed]
172. Feng, W.; Ji, P. Enzymes immobilized on carbon nanotubes. *Biotechnol. Adv.* **2011**, *29*, 889–895. [CrossRef]
173. Bijoy, G.; Rajeev, R.; Benny, L.; Jose, S.; Varghese, A. Enzyme immobilization on biomass-derived carbon materials as a sustainable approach towards environmental applications. *Chemosphere* **2022**, *307*, 135759. [CrossRef] [PubMed]
174. Souza Júnior, E.C.; Santos, M.P.F.; Sampaio, V.S.; Ferrão, S.P.B.; Fontan, R.C.I.; Bonomo, R.C.F.; Veloso, C.M. Hydrolysis of casein from different sources by immobilized trypsin on biochar: Effect of immobilization method. *J. Chromatogr. B* **2020**, *1146*, 122124. [CrossRef] [PubMed]
175. Han, H.; Song, P.; Cai, Z.; Dong, W.; Khan, A.; Yang, K.; Fang, Y.; Liu, P.; Mašek, O.; Li, X. Immobilizing chromate reductase NfoR on magnetic biochar reduced Cr(VI) in copper-containing wastewater. *J. Clean. Prod.* **2022**, *361*, 132118. [CrossRef]
176. Liu, J.-J.; Kim, J.-G.; Kim, H.-B.; Abeysinghe, S.; Lin, Y.-W.; Baek, K. Covalent immobilizing horseradish peroxidase on electrochemically-functionalized biochar for phenol removal. *Chemosphere* **2023**, *312*, 137218. [CrossRef]
177. Petronijević, M.; Panić, S.; Savić, S.; Agbaba, J.; Molnar Jazić, J.; Milanović, M.; Đurišić-Mladenović, N. Characterization and application of biochar-immobilized crude horseradish peroxidase for removal of phenol from water. *Colloids Surf. B Biointerfaces* **2021**, *208*, 112038. [CrossRef]
178. Jiang, Q.; Fang, R.; Gul, I.; Aer, L.; Zhao, Y.; Guo, J.; Tang, L. Halohydrin dehalogenase immobilization in magnetic biochar for sustainable halocarbon biodegradation and biotransformation. *Environ. Technol. Innov.* **2022**, *27*, 102759. [CrossRef]
179. Kyere-Yeboah, K.; Bique, I.K.; Qiao, X.-c. Advances of non-thermal plasma discharge technology in degrading recalcitrant wastewater pollutants. A comprehensive review. *Chemosphere* **2023**, *320*, 138061. [CrossRef] [PubMed]
180. Bello, M.M.; Raman, A.A.A.; Asghar, A. A review on approaches for addressing the limitations of Fenton oxidation for recalcitrant wastewater treatment. *Process Saf. Environ. Prot.* **2019**, *126*, 119–140. [CrossRef]
181. Morsi, R.; Bilal, M.; Iqbal, H.M.; Ashraf, S.S. Laccases and peroxidases: The smart, greener and futuristic biocatalytic tools to mitigate recalcitrant emerging pollutants. *Sci. Total Environ.* **2020**, *714*, 136572. [CrossRef] [PubMed]
182. Majeau, J.-A.; Brar, S.K.; Tyagi, R.D. Laccases for removal of recalcitrant and emerging pollutants. *Bioresour. Technol.* **2010**, *101*, 2331–2350. [CrossRef] [PubMed]
183. Yaropolov, A.; Skorobogat'Ko, O.; Vartanov, S.; Varfolomeyev, S. Laccase: Properties, catalytic mechanism, and applicability. *Appl. Biochem. Biotechnol.* **1994**, *49*, 257–280. [CrossRef]
184. Hoinacki da Silva, C.K.; Polidoro, A.S.; Cabrera Ruschel, P.M.; Thue, P.S.; Jacques, R.A.; Lima, É.C.; Bussamara, R.; Fernandes, A.N. Laccase covalently immobilized on avocado seed biochar: A high-performance biocatalyst for acetaminophen sorption and biotransformation. *J. Environ. Chem. Eng.* **2022**, *10*, 107731. [CrossRef]
185. Zou, M.; Tian, W.; Chu, M.; Lu, Z.; Liu, B.; Xu, D. Magnetically separable laccase-biochar composite enable highly efficient adsorption-degradation of quinolone antibiotics: Immobilization, removal performance and mechanisms. *Sci. Total Environ.* **2023**, *879*, 163057. [CrossRef]
186. Imam, A.; Suman, S.K.; Singh, R.; Vempatapu, B.P.; Ray, A.; Kanaujia, P.K. Application of laccase immobilized rice straw biochar for anthracene degradation. *Environ. Pollut.* **2021**, *268*, 115827. [CrossRef]

187. Pandey, D.; Daverey, A.; Dutta, K.; Arunachalam, K. Bioremoval of toxic malachite green from water through simultaneous decolorization and degradation using laccase immobilized biochar. *Chemosphere* **2022**, *297*, 134126. [CrossRef]
188. Pandey, D.; Daverey, A.; Dutta, K.; Arunachalam, K. Dye removal from simulated and real textile effluent using laccase immobilized on pine needle biochar. *J. Water Process Eng.* **2023**, *53*, 103710. [CrossRef]
189. Zhang, H.; Hay, A.G. Magnetic biochar derived from biosolids via hydrothermal carbonization: Enzyme immobilization, immobilized-enzyme kinetics, environmental toxicity. *J. Hazard. Mater.* **2020**, *384*, 121272. [CrossRef] [PubMed]
190. Wang, Z.; Ren, D.; Zhang, X.; Zhang, S.; Chen, W. Adsorption-degradation of malachite green using alkali-modified biochar immobilized laccase under multi-methods. *Adv. Powder Technol.* **2022**, *33*, 103821. [CrossRef]
191. Aliakbarinodehi, N.; Taurino, I.; Pravin, J.; Tagliaferro, A.; Piccinini, G.; De Micheli, G.; Carrara, S. Electrochemical nanostructured biosensors: Carbon nanotubes versus conductive and semi-conductive nanoparticles. *Chem. Pap.* **2015**, *69*, 134–142. [CrossRef]
192. Kim, J.; Oh, Y.; Shin, J.; Yang, M.; Shin, N.; Shekhar, S.; Hong, S. Nanoscale mapping of carrier mobilities in the ballistic transports of carbon nanotube networks. *ACS Nano* **2022**, *16*, 21626–21635. [CrossRef] [PubMed]
193. Du, X.; Skachko, I.; Barker, A.; Andrei, E.Y. Approaching ballistic transport in suspended graphene. *Nat. Nanotechnol.* **2008**, *3*, 491–495. [CrossRef] [PubMed]
194. Wan, Z.; Sun, Y.; Tsang, D.C.; Hou, D.; Cao, X.; Zhang, S.; Gao, B.; Ok, Y.S. Sustainable remediation with an electroactive biochar system: Mechanisms and perspectives. *Green Chem.* **2020**, *22*, 2688–2711. [CrossRef]
195. Giorcelli, M.; Bartoli, M.; Sanginario, A.; Padovano, E.; Rosso, C.; Rovere, M.; Tagliaferro, A. High-Temperature Annealed Biochar as a Conductive Filler for the Production of Piezoresistive Materials for Energy Conversion Application. *ACS Appl. Electron. Mater.* **2021**, *3*, 838–844. [CrossRef]
196. Jagdale, P.; Nair, J.R.; Khan, A.; Armandi, M.; Meligrana, G.; Hernandez, F.R.; Rusakova, I.; Piatti, E.; Rovere, M.; Tagliaferro, A.; et al. Waste to life: Low-cost, self-standing, 2D carbon fiber green Li-ion battery anode made from end-of-life cotton textile. *Electrochim. Acta* **2021**, *368*, 137644. [CrossRef]
197. Anglada, A.; Urtiaga, A.; Ortiz, I. Contributions of electrochemical oxidation to waste-water treatment: Fundamentals and review of applications. *J. Chem. Technol. Biotechnol.* **2009**, *84*, 1747–1755. [CrossRef]
198. Canizares, P.; Paz, R.; Lobato, J.; Sáez, C.; Rodrigo, M. Electrochemical treatment of the effluent of a fine chemical manufacturing plant. *J. Hazard. Mater.* **2006**, *138*, 173–181. [CrossRef] [PubMed]
199. Han, W.-Q.; Wang, L.-J.; Sun, X.-Y.; Li, J.-S. Treatment of bactericide wastewater by combined process chemical coagulation, electrochemical oxidation and membrane bioreactor. *J. Hazard. Mater.* **2008**, *151*, 306–315. [CrossRef] [PubMed]
200. Cho, S.-H.; Lee, H.-J.; Moon, S.-H. Integrated electroenzymatic and electrochemical treatment of petrochemical wastewater using a pilot scale membraneless system. *Process Biochem.* **2008**, *43*, 1371–1376. [CrossRef]
201. El-Ashtoukhy, E.-S.; Amin, N.; Abdelwahab, O. Treatment of paper mill effluents in a batch-stirred electrochemical tank reactor. *Chem. Eng. J.* **2009**, *146*, 205–210. [CrossRef]
202. Rajkumar, D.; Palanivelu, K. Electrochemical treatment of industrial wastewater. *J. Hazard. Mater.* **2004**, *113*, 123–129. [CrossRef] [PubMed]
203. Rodrigo, M.; Cañizares, P.; Buitrón, C.; Sáez, C. Electrochemical technologies for the regeneration of urban wastewaters. *Electrochim. Acta* **2010**, *55*, 8160–8164. [CrossRef]
204. Werkneh, A.A.; Beyene, H.D.; Osunkunle, A.A. Recent advances in brewery wastewater treatment; approaches for water reuse and energy recovery: A review. *Environ. Sustain.* **2019**, *2*, 199–209. [CrossRef]
205. Piya-Areetham, P.; Shenchunthichai, K.; Hunsom, M. Application of electrooxidation process for treating concentrated wastewater from distillery industry with a voluminous electrode. *Water Res.* **2006**, *40*, 2857–2864. [CrossRef]
206. Waterston, K.; Wang, J.W.; Bejan, D.; Bunce, N.J. Electrochemical waste water treatment: Electrooxidation of acetaminophen. *J. Appl. Electrochem.* **2006**, *36*, 227–232. [CrossRef]
207. Ansari, M.N.; Sarrouf, S.; Ehsan, M.F.; Manzoor, S.; Ashiq, M.N.; Alshawabkeh, A.N. Polarity reversal for enhanced in-situ electrochemical synthesis of H_2O_2 over banana-peel derived biochar cathode for water remediation. *Electrochim. Acta* **2023**, *453*, 142351. [CrossRef]
208. Kim, J.-G.; Kim, H.-B.; Baek, K. Novel electrochemical method to activate biochar derived from spent coffee grounds for enhanced adsorption of lead (Pb). *Sci. Total Environ.* **2023**, *886*, 163891. [CrossRef] [PubMed]
209. Kim, J.-G.; Sarrouf, S.; Ehsan, M.F.; Baek, K.; Alshawabkeh, A.N. In-situ hydrogen peroxide formation and persulfate activation over banana peel-derived biochar cathode for electrochemical water treatment in a flow reactor. *Chemosphere* **2023**, *331*, 138849. [CrossRef] [PubMed]
210. Dai, J.; Wang, Z.; Chen, K.; Ding, D.; Yang, S.; Cai, T. Applying a novel advanced oxidation process of biochar activated periodate for the efficient degradation of bisphenol A: Two nonradical pathways. *Chem. Eng. J.* **2023**, *453*, 139889. [CrossRef]
211. Mezza, A.; Bartoli, M.; Chiodoni, A.; Zeng, J.; Pirri, C.F.; Sacco, A. Optimizing the Performance of Low-Loaded Electrodes for CO_2-to-CO Conversion Directly from Capture Medium: A Comprehensive Parameter Analysis. *Nanomaterials* **2023**, *13*, 2314. [CrossRef] [PubMed]
212. Jin, S.; Hao, Z.; Zhang, K.; Yan, Z.; Chen, J. Advances and challenges for the electrochemical reduction of CO_2 to CO: From fundamentals to industrialization. *Angew. Chem.* **2021**, *133*, 20795–20816. [CrossRef]
213. Shen, J.; Kolb, M.J.; Gottle, A.J.; Koper, M.T. DFT study on the mechanism of the electrochemical reduction of CO_2 catalyzed by cobalt porphyrins. *J. Phys. Chem. C* **2016**, *120*, 15714–15721. [CrossRef]

214. Singh, M.R.; Goodpaster, J.D.; Weber, A.Z.; Head-Gordon, M.; Bell, A.T. Mechanistic insights into electrochemical reduction of CO_2 over Ag using density functional theory and transport models. *Proc. Natl. Acad. Sci. USA* **2017**, *114*, E8812–E8821. [CrossRef]
215. Rosen, J.; Hutchings, G.S.; Lu, Q.; Rivera, S.; Zhou, Y.; Vlachos, D.G.; Jiao, F. Mechanistic insights into the electrochemical reduction of CO_2 to CO on nanostructured Ag surfaces. *ACS Catal.* **2015**, *5*, 4293–4299. [CrossRef]
216. Gattrell, M.; Gupta, N.; Co, A. A review of the aqueous electrochemical reduction of CO_2 to hydrocarbons at copper. *J. Electroanal. Chem.* **2006**, *594*, 1–19. [CrossRef]
217. Lourenço, M.A.O.; Zeng, J.; Jagdale, P.; Castellino, M.; Sacco, A.; Farkhondehfal, M.A.; Pirri, C.F. Biochar/Zinc Oxide Composites as Effective Catalysts for Electrochemical CO_2 Reduction. *ACS Sustain. Chem. Eng.* **2021**, *9*, 5445–5453. [CrossRef]
218. Wenderich, K.; Mul, G. Methods, mechanism, and applications of photodeposition in photocatalysis: A review. *Chem. Rev.* **2016**, *116*, 14587–14619. [CrossRef]
219. Franceschini, F.; Jagdale, P.; Bartoli, M.; Tagliaferro, A. Perspectives on the use of bismuth-based materials for sensing and removal of water pollutants. *Curr. Opin. Environ. Sci. Health* **2022**, *26*, 100345. [CrossRef]
220. Candish, L.; Collins, K.D.; Cook, G.C.; Douglas, J.J.; Gómez-Suárez, A.; Jolit, A.; Keess, S. Photocatalysis in the life science industry. *Chem. Rev.* **2021**, *122*, 2907–2980. [CrossRef] [PubMed]
221. Ombaka, L.M.; McGettrick, J.D.; Oseghe, E.O.; Al-Madanat, O.; Genannt Best, F.R.; Msagati, T.A.; Davies, M.L.; Bredow, T.; Bahnemann, D.W. Photocatalytic H2 production and degradation of aqueous 2-chlorophenol over B/N-graphene-coated Cu0/TiO2: A DFT, experimental and mechanistic investigation. *J. Environ. Manag.* **2022**, *311*, 114822. [CrossRef] [PubMed]
222. Mian, M.M.; Liu, G. Recent progress in biochar-supported photocatalysts: Synthesis, role of biochar, and applications. *RSC Adv.* **2018**, *8*, 14237–14248. [CrossRef] [PubMed]
223. Cui, J.; Zhang, F.; Li, H.; Cui, J.; Ren, Y.; Yu, X. Recent Progress in Biochar-Based Photocatalysts for Wastewater Treatment: Synthesis, Mechanisms, and Applications. *Appl. Sci.* **2020**, *10*, 1019. [CrossRef]
224. Bhavani, P.; Hussain, M.; Park, Y.-K. Recent advancements on the sustainable biochar based semiconducting materials for photocatalytic applications: A state of the art review. *J. Clean. Prod.* **2022**, *330*, 129899. [CrossRef]
225. Feng, X.; Li, X.; Su, B.; Ma, J. Solid-phase fabrication of TiO2/Chitosan-biochar composites with superior UV–vis light driven photocatalytic degradation performance. *Colloids Surf. A Physicochem. Eng. Asp.* **2022**, *648*, 129114. [CrossRef]
226. Kim, J.R.; Kan, E. Heterogeneous photocatalytic degradation of sulfamethoxazole in water using a biochar-supported TiO_2 photocatalyst. *J. Environ. Manag.* **2016**, *180*, 94–101. [CrossRef]
227. Thuan, D.V.; Chu, T.T.H.; Thanh, H.D.T.; Le, M.V.; Ngo, H.L.; Le, C.L.; Thi, H.P. Adsorption and photodegradation of micropollutant in wastewater by photocatalyst TiO2/rice husk biochar. *Environ. Res.* **2023**, *236*, 116789. [CrossRef]
228. Xie, Y.; Liu, A.; Bandala, E.R.; Goonetilleke, A. TiO2-biochar composites as alternative photocatalyst for stormwater disinfection. *J. Water Process Eng.* **2022**, *48*, 102913. [CrossRef]
229. Zahedifar, M.; Seyedi, N. Bare 3D-TiO_2/magnetic biochar dots (3D-TiO_2/BCDs MNPs): Highly efficient recyclable photocatalyst for diazinon degradation under sunlight irradiation. *Phys. E Low-Dimens. Syst. Nanostruct.* **2022**, *139*, 115151. [CrossRef]
230. Amir, M.; Fazal, T.; Iqbal, J.; Din, A.A.; Ahmed, A.; Ali, A.; Razzaq, A.; Ali, Z.; Rehman, M.S.U.; Park, Y.-K. Integrated adsorptive and photocatalytic degradation of pharmaceutical micropollutant, ciprofloxacin employing biochar-ZnO composite photocatalysts. *J. Ind. Eng. Chem.* **2022**, *115*, 171–182. [CrossRef]
231. Gonçalves, N.P.F.; Lourenço, M.A.O.; Baleuri, S.R.; Bianco, S.; Jagdale, P.; Calza, P. Biochar waste-based ZnO materials as highly efficient photocatalysts for water treatment. *J. Environ. Chem. Eng.* **2022**, *10*, 107256. [CrossRef]
232. An, M.; Yang, Z.; Zhang, B.; Xue, B.; Xu, G.; Chen, W.; Wang, S. Construction of biochar-modified TiO_2 anatase-rutile phase S-scheme heterojunction for enhanced performance of photocatalytic degradation and photocatalytic hydrogen evolution. *J. Environ. Chem. Eng.* **2023**, *11*, 110367. [CrossRef]
233. Chakhtouna, H.; Ouhssain, A.; Kadmiri, I.M.; Benzeid, H.; Zari, N.; Qaiss, A.e.k.; Bouhfid, R. Photocatalytic and bactericidal behaviors of Ag/TiO2 doped biochar through Ball–milling approach. *J. Photochem. Photobiol. A Chem.* **2023**, *444*, 114971. [CrossRef]
234. Feng, X.; Li, X.; Su, B.; Ma, J. Two-step construction of WO3@TiO2/CS-biochar S-scheme heterojunction and its synergic adsorption/photocatalytic removal performance for organic dye and antibiotic. *Diam. Relat. Mater.* **2023**, *131*, 109560. [CrossRef]
235. Herath, A.; Navarathna, C.; Warren, S.; Perez, F.; Pittman, C.U.; Mlsna, T.E. Iron/titanium oxide-biochar (Fe_2TiO_5/BC): A versatile adsorbent/photocatalyst for aqueous Cr(VI), Pb2+, F- and methylene blue. *J. Colloid Interface Sci.* **2022**, *614*, 603–616. [CrossRef]
236. Li, H.; Hu, J.; Zhou, X.; Li, X.; Wang, X. An investigation of the biochar-based visible-light photocatalyst via a self-assembly strategy. *J. Environ. Manag.* **2018**, *217*, 175–182. [CrossRef]
237. Huang, L.; Liu, H.; Wang, Y.; Zhang, T.C.; Yuan, S. Construction of ternary Bi_2O_3/biochar/g-C3N4 heterojunction to accelerate photoinduced carrier separation for enhanced tetracycline photodegradation. *Appl. Surf. Sci.* **2023**, *616*, 156509. [CrossRef]
238. Qi, K.; Wang, Z.; Xie, X.; Wang, Z. Photocatalytic performance of pyrochar and hydrochar in heterojunction photocatalyst for organic pollutants degradation: Activity comparison and mechanism insight. *Chem. Eng. J.* **2023**, *467*, 143424. [CrossRef]
239. Li, S.; Wang, Z.; Xie, X.; Liang, G.; Cai, X.; Zhang, X.; Wang, Z. Fabrication of vessel–like biochar–based heterojunction photocatalyst Bi2S3/BiOBr/BC for diclofenac removal under visible LED light irradiation: Mechanistic investigation and intermediates analysis. *J. Hazard. Mater.* **2020**, *391*, 121407. [CrossRef]
240. Li, S.; Wang, Z.; Zhao, X.; Yang, X.; Liang, G.; Xie, X. Insight into enhanced carbamazepine photodegradation over biochar-based magnetic photocatalyst Fe_3O_4/BiOBr/BC under visible LED light irradiation. *Chem. Eng. J.* **2019**, *360*, 600–611. [CrossRef]

241. Yang, Q.; Li, X.; Tian, Q.; Pan, A.; Liu, X.; Yin, H.; Shi, Y.; Fang, G. Synergistic effect of adsorption and photocatalysis of BiOBr/lignin-biochar composites with oxygen vacancies under visible light irradiation. *J. Ind. Eng. Chem.* **2023**, *117*, 117–129. [CrossRef]
242. Zhang, X.; Wu, Z.; Wu, Y.; Giwa, A.S.; Huang, S.; Niu, L. Visible-light-driven simultaneous decontamination of multi-antibiotics by facile synthesized BiOCl loaded food wastes biochar. *Environ. Pollut.* **2023**, *316*, 120683. [CrossRef]
243. Wang, T.; Cai, J.; Zheng, J.; Fang, K.; Hussain, I.; Husein, D.Z. Facile synthesis of activated biochar/BiVO4 heterojunction photocatalyst to enhance visible light efficient degradation for dye and antibiotics: Applications and mechanisms. *J. Mater. Res. Technol.* **2022**, *19*, 5017–5036. [CrossRef]
244. Zhang, X.; Guo, M.; Liu, S.; Xiang, H.; Guo, X.; Yang, Y. Performance and mechanism of biochar-coupled BiVO4 photocatalyst on the degradation of sulfanilamide. *J. Clean. Prod.* **2021**, *325*, 129349. [CrossRef]
245. Luo, S.; Li, S.; Zhang, S.; Cheng, Z.; Nguyen, T.T.; Guo, M. Visible-light-driven Z-scheme protonated g-C_3N_4/wood flour biochar/$BiVO_4$ photocatalyst with biochar as charge-transfer channel for enhanced RhB degradation and Cr(VI) reduction. *Sci. Total Environ.* **2022**, *806*, 150662. [CrossRef]
246. Deng, C.; Peng, L.; Ling, X.; Wang, T.; Xu, R.; Zhu, Y.; Wang, C.; Qian, X.; Wang, L.; Wu, Y.; et al. Construction of S-scheme Zn0.2Cd0.8S/biochar aerogel architectures for boosting photocatalytic hydrogen production under sunlight irradiation. *J. Clean. Prod.* **2023**, *414*, 137616. [CrossRef]
247. Chen, Z.; He, Z.; Zhou, M.; Xie, M.; He, T.; Zhao, Y.; Chen, X.; Wu, Y.; Xu, Z. In-situ synthesis of biochar modified $PbMoO_4$: An efficient visible light-driven photocatalyst for tetracycline removal. *Chemosphere* **2021**, *284*, 131260. [CrossRef]
248. Kumar Ray, S.; Anil Kumar Reddy, P.; Yoon, S.; Shin, J.; Chon, K.; Bae, S. A magnetically separable α-$NiMoO_4$/$ZnFe_2O_4$/coffee biochar heterojunction photocatalyst for efficient ketoprofen degradation. *Chem. Eng. J.* **2023**, *452*, 139546. [CrossRef]
249. Chu, S.; Cui, Y.; Liu, N. The path towards sustainable energy. *Nat. Mater.* **2017**, *16*, 16–22. [CrossRef] [PubMed]
250. Cao, X.; Sun, S.; Sun, R. Application of biochar-based catalysts in biomass upgrading: A review. *RSC Adv.* **2017**, *7*, 48793–48805. [CrossRef]
251. Yao, D.; Hu, Q.; Wang, D.; Yang, H.; Wu, C.; Wang, X.; Chen, H. Hydrogen production from biomass gasification using biochar as a catalyst/support. *Bioresour. Technol.* **2016**, *216*, 159–164. [CrossRef] [PubMed]
252. Bhakta, A.K.; Fiorenza, R.; Jlassi, K.; Mekhalif, Z.; Ali, A.M.A.; Chehimi, M.M. The emerging role of biochar in the carbon materials family for hydrogen production. *Chem. Eng. Res. Des.* **2022**, *188*, 209–228. [CrossRef]
253. Jafri, N.; Wong, W.; Doshi, V.; Yoon, L.; Cheah, K.H. A review on production and characterization of biochars for application in direct carbon fuel cells. *Process Saf. Environ. Prot.* **2018**, *118*, 152–166. [CrossRef]
254. Gianola, G.; Garino, N.; Bartoli, M.; Sacco, A.; Pirri, C.F.; Zeng, J. Microwave-assisted synthesis of N/S-doped CNC/SnO_2 nanocomposite as a promising catalyst for oxygen reduction in alkaline media. *Mater. Chem. Phys.* **2023**, *308*, 128205. [CrossRef]
255. Zhang, F.; Miao, J.; Liu, W.; Xu, D.; Li, X. Heteroatom embedded graphene-like structure anchored on porous biochar as efficient metal-free catalyst for ORR. *Int. J. Hydrogen Energy* **2019**, *44*, 30986–30998. [CrossRef]
256. Zago, S.; Bartoli, M.; Muhyuddin, M.; Vanacore, G.M.; Jagdale, P.; Tagliaferro, A.; Santoro, C.; Specchia, S. Engineered biochar derived from pyrolyzed waste tea as a carbon support for Fe-NC electrocatalysts for the oxygen reduction reaction. *Electrochim. Acta* **2022**, *412*, 140128. [CrossRef]
257. Chakraborty, I.; Sathe, S.; Dubey, B.; Ghangrekar, M. Waste-derived biochar: Applications and future perspective in microbial fuel cells. *Bioresour. Technol.* **2020**, *312*, 123587. [CrossRef]
258. Li, S.; Ho, S.-H.; Hua, T.; Zhou, Q.; Li, F.; Tang, J. Sustainable biochar as an electrocatalysts for the oxygen reduction reaction in microbial fuel cells. *Green Energy Environ.* **2021**, *6*, 644–659. [CrossRef]
259. Zhou, X.; Jin, H.; Ma, Z.; Li, N.; Li, G.; Zhang, T.; Lu, P.; Gong, X. Biochar sacrificial anode assisted water electrolysis for hydrogen production. *Int. J. Hydrogen Energy* **2022**, *47*, 36482–36492. [CrossRef]
260. Ying, Z.; Geng, Z.; Zheng, X.; Dou, B.; Cui, G. Improving water electrolysis assisted by anodic biochar oxidation for clean hydrogen production. *Energy* **2022**, *238*, 121793. [CrossRef]
261. Igalavithana, A.D.; You, S.; Zhang, L.; Shang, J.; Lehmann, J.; Wang, X.; Zhu, Y.-G.; Tsang, D.C.; Park, Y.-K.; Hou, D. Progress, barriers, and prospects for achieving a "Hydrogen Society" and opportunities for biochar technology. *ACS EST Eng.* **2022**, *2*, 1987–2001. [CrossRef]
262. Verheijen, F.G.; Bastos, A.C.; Schmidt, H.-P.; Jeffery, S. Biochar and certification 1. In *Sustainability Certification Schemes in the Agricultural and Natural Resource Sectors*; Routledge: Abingdon, UK, 2019; pp. 113–136.
263. Woolf, D.; Amonette, J.E.; Street-Perrott, F.A.; Lehmann, J.; Joseph, S. Sustainable biochar to mitigate global climate change. *Nat. Commun.* **2010**, *1*, 56. [CrossRef] [PubMed]